In silico analysis of novel mutation K96R in *M.tuberculosis* PncA: Computational characterization of Pyrazinamide drug resistance mechanism and development of novel drug leads to combat mutations in PncA

A Major Project dissertation submitted

in partial fulfilment of the requirement for the degree of

Master of Technology
In
Bioinformatics

Submitted by

Chakshu Vats

(2K12/BIO/05)

Delhi Technological University, Delhi, India

Under the supervision of
Dr. Navneeta Bharadvaja

Department of Biotechnology
Delhi Technological University
(Formerly Delhi College of Engineering)
Shahbad Daulatpur, Main Bawana Road,
Delhi-110042, INDIA

CERTIFICATE

This is to certify that the M. Tech. dissertation entitled **"*In silico* analysis of novel mutation K96R in *M.tuberculosis* PncA: Computational characterization of Pyrazinamide drug resistance mechanism and development of novel drug leads to combat mutations in PncA"**, submitted by **CHAKSHU VATS (2K12/BIO/05)** in partial fulfilment of the requirement for the award of the degree of Master of Engineering, Delhi Technological University (Formerly Delhi College of Engineering, University of Delhi), is an authentic record of the candidate's own work carried out by her under my guidance.

The information and data enclosed in this dissertation is original and has not been submitted elsewhere for honouring of any other degree.

Date:

Navneeta Bharadvaja
(Project Mentor)
Department of Bio-Technology
Delhi Technological University
(Formerly Delhi College of Engineering, University of Delhi)

DECLARATION

I, **Chakshu Vats**, hereby declare that the work entitled **"*In silico* analysis of novel mutation K96R in *M.tuberculosis* PncA: Computational characterization of Pyrazinamide drug resistance mechanism and development of novel drug leads to combat mutations in PncA"** has been carried out by me under the guidance of Dr Navneeta Bharadvaja, in Delhi Technological University, Delhi.

This dissertation is part of partial fulfilment of requirement for the degree of M.Tech in Bioinformatics. This is the original work and has not been submitted for any other degree in any other university.

Chakshu Vats

Roll No.: 2K12/BIO/05

ACKNOWLEDGEMENT

I would like to acknowledge my deep sense of gratitude to ***Prof. B.D. Malhotra, (Head of Department) Department of Biotechnology, Delhi Technological University, Delhi-110042*** *for giving me an opportunity to study and work in this prestigious Institute.*

I am extremely thankful to my mentor, ***Dr. Navneeta Bharadvaja****,* ***Assistant professor, Department of Biotechnology, Delhi Technological University, Delhi-110042*** *for her exemplary guidance, monitoring and constant encouragement throughout the M. Tech course. I would also like to thank her for sparing the efforts in compiling the work presented here.*

I wish to express my sincere gratitude to ***Dr. Abhinav Grover, Assistant Professor, School of Biotechnology, Jawaharlal Nehru University, Delhi-110067*** *for providing me continuous support throughout this project.*

At last, I am extremely thankful to my parents, family members and friends whose blessings and support were always with me.

Chakshu Vats
2K12/BIO/05

CONTENTS

LIST OF FIGURES AND TABLES

LIST OF ABBREVIATIONS

AIDS	Acquired Immunodeficiency Syndrome
AMK	Amikacin
BCG	Bacillus of Calmette and Guérin
CAP	Capreomycin
DNA	Deoxyribonucleic Acid
DR-TB	Drug resistant Tuberculosis
EIS	Enhanced Intracellular Survival
INH	Isoniazid
HBC	High Burden Countries
HIV	Human Immunodeficiency Virus
HTVS	High Throughput Virtual Screening
KAN	Kanamycin
L-BFGS	Low-memory Broyden- Fletcher- Goldfarb Shanno quasi-Newtonian minimiser
MD	Molecular Dynamics
MRSA	Meticillin resistant *Staphylococcus aureus*
MtPncA	Mycobacterial Pyrazinamidase
NGS	Next Generation Sequencing
OPLS	Optimized Potentials for Liquid Simulations
PBP	Penicillin binding proteins
PDB	Protein Data Bank
PncA	Pyrazinamidase
POC	pyrazonic acid
PPC	N-phenylpyrazine-2-carboxamide
PZA	Pyrazinamide
RMP	Rifampicin

RMSD	Root Mean Square Deviation
RMSF	Root Mean Square Fluctuations
RNA	Ribonucleic Acid
TB	Tuberculosis
TDR	Totally Drug Resistant
WHO	World Health Organisation
XP	Extra Precision Docking

In silico analysis of novel mutation K96R in *M.tuberculosis* PncA: Computational characterization of Pyrazinamide drug resistance mechanism and development of novel drug leads to combat mutations in PncA

Chakshu Vats

Delhi Technological University, Delhi, India

ABSTRACT

Pyrazinamide (PZA) is one of the most effective first line treatments against tuberculosis disease. The drug is capable of bacteriostatic action and also acts on bacterial spores which eliminate chances of resurfacing of the infection. However, in recent years the there has been a major increase in the occurrence of drug resistant bacterial strains. These mutations prevents drug binding to bacterial proteins and impart resistance. Resistance against PZA is caused by mutations in PncA protein which is the activator of the prodrug PZA. Resistance has been developed against many first and second line drugs and cases of Multi Drug Resistance are on the rise. In order to develop better drug therapies it is imperative to first understand the mechanism of action of these drug resistance causing mutations. In the present study, we have tried to gain insight into the mechanism of action of a novel mutation K96R occurring in the PncA catalytic region. For this purpose, binding cavity assessment was performed to identify the change in volume after mutation. This gives us an idea about how the ligand would be perceived in the cavity. This was followed by docking studies to analyse the binding of the ligand with the protein, binding energies, vander waal energies and electrostatic energies. Interaction networks of both native and mutant protein with PZA ligand were also analyzed. To identify the dynamic conformational changes in the complexes, molecular dynamic simulations were performed. These results helped in developing a combinatorial library of novel PZA derivatives. Later, virtual screening was performed with novel pyrazinamide derivatives to identify leads which were capable of binding with wild and various PncA mutants with greater efficacy than PZA.

Keywords: Tuberculosis, PZA, PncA, mutations, drug resistance, Molecular Dynamics, Virtual Screening

INTRODUCTION

Historically, tuberculosis (TB) has been credited as mankind's biggest infectious killer. Evidence suggests that TB infection dates back to nine millennia specifically to a Neolithic Eastern Mediterranean settlement (Hershkovitz et al., 2008). It was a pre-antibiotic era the disease caused a certain death to all the infected beings. With the advent of anti-biotic in 20th century, the disease was listed as a curable disease. The discovery of causative *M.tuberculosis* by Robert Koch in 1982 and its curable identity led to a decline in interest in the disease as a whole until 1980's, when the disease returned with vengeance. Tuberculosis has returned as one of the most grievous infectious diseases. Unprecedented use of antibiotics has resulted in the emergence of drug resistant strains of *M. tuberculosis* (Dye, 2000). The accumulation of resistance mutations has given rise to the rapid evolution of *M. tuberculosis* strains that are multidrug resistant (MDR), extensively drug resistant (XDR), or more recently, totally drug resistant (TDR).

About one third of the world population is known to be suffering from the infection caused by *M.tuberculosis*. In 2008, 1.3 million deaths were reported owing to this infection (McQuade Billingsley et al., 2011). The growth of drug resistant bacteria has attracted scientists all over the world to ponder upon this issue for more research. The emergence of drug-resistant strains is one of the main causes for the current spread of TB (Heifets and Cangelosi, 1999). All the first line drugs have their share of resistant genes. Research has shown the mechanism of action in some cases as with 315th position mutation in INH leading to resistance in Isoniazid. However, a lot of new mutations are emerging rapidly. Pyrazinamide (PZA), a derivative of nicotinamide is one of the most imperative first-line drug treatments against tuberculosis (Wright et al., 2009). The drug PZA is significantly used in MDR tuberculosis in combination with isoniazid, rifampicin and ethambutol in regimens. The most potent action of the drug is against the semi-dormant bacilli in an acidic environment, which cannot be treated with most other drugs and thus shortens the chemotherapy period. Emergence of drug resistant strains of tuberculosis is one of the major concerns being faced by both developed and developing countries. Several mutations have been identified in Mtb proteins making them resistant to current drug therapies. Mutations in PncA play a major role behind PZA resistance in M. tuberculosis (Jureen et al., 2008; Lemaitre et al., 1999; Morlock et al., 2000; Pandey et al., 2009; Scorpio et al., 1997; Sheen et al., 2012; Sreevatsan et al., 1997).

With the rise in the mutations it becomes difficult to focus on ever rising mutations quickly and efficiently (Dalton et al., 2012). Therefore *in silico* based studies are proving to be a method of choice for most researches. Critical understanding of these mechanisms allows the development of robust and efficient molecular diagnostic tests and provides a platform for the development of new drugs. Another method can be improvising the existing drugs. This would lead to faster and efficient development of the drug (Dooley et al., 2012). A study was performed by Daum et al, to identify the novel mutations associated with PZA resistance. In order to perform NGS, 26 random samples of South African origin were selected which were diagnosed with either MDR or XDR TB. Nine out of 26 were found to be PZA resistant. Using ion torrent method, the sequence of 9 patients was studied and it was observed that all

of them contained one of the mutations conferring resistance. This methodology revealed the novel mutation Lys-96-Arg. The method provides advantage over other existing methods due to the depth of coverage or deep sequencing.

Objectives of this study

With the ever increasing population and infections TB continues to be a prominent disease both in developing and developed. In our study a novel mutation Lys-96-Arg (K96R) is considered. This mutation has been revealed by deep sequencing via NGS (Next Generation sequencing) in the *pncA* gene (Daum et al., 2014). The position spans the active centre of the protein and thereby is of utmost importance (Petrella et al., 2011).Based on this, we have briefly outlined the objectives of the experiment.

- To identify the mechanism of resistance underlying K96R mutation in *pncA* gene.
- Based on the mechanism, creating a combinatorial library of novel PZA derivatives p
- To perform High throughput virtual screening to identify a lead compound that could bind to both wild and mutant protein.
- To present inhibition mechanism for the proposed lead compound

Besides efforts to find new drugs, both development of novel alternative therapeutics and improvement of the current therapies will be required for the successful fight against the spreading epidemic of drug resistant TB. Methods for pharmaceutical inhibition of resistance mechanisms will play a significant role in this new age of antibiotic development. This approach would not only help to protect the efficacy of the current TB drugs but also boost the anti-TB activity of the existing TB- and non-TB drugs, ultimately broadening the therapeutic options for TB treatment.

FLOWCHART OF THE WORK

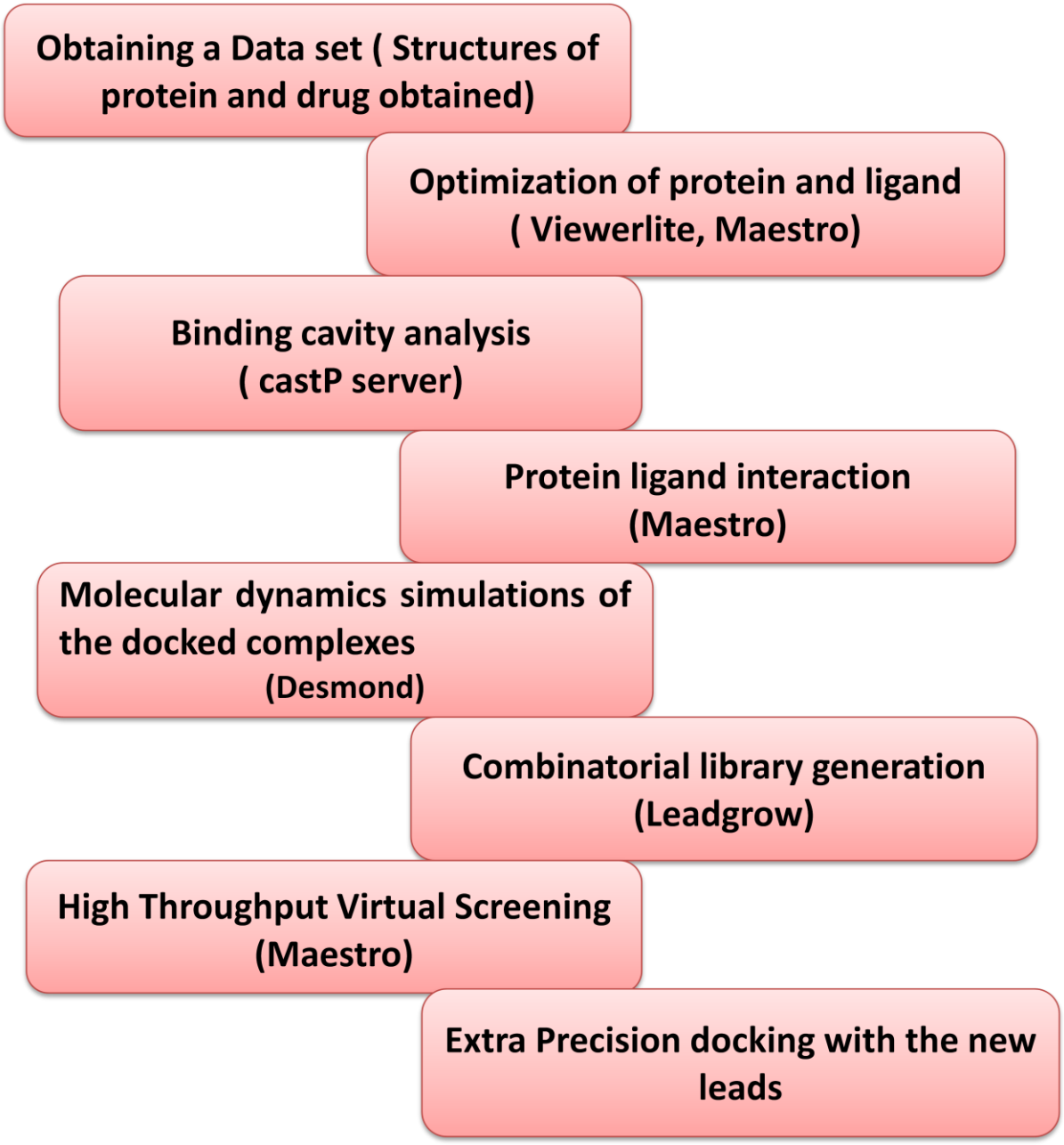

Figure 1: Workflow of the experiment and tools used

REVIEW OF LITERATURE

3.1 Tuberculosis

Tuberculosis or TB (short for tubercle bacillus), is a typical, and by and large deadly, irresistible infection brought about by different strains of mycobacteria, generally *M.tuberculosis*. In the past it was additionally called phthisis, phthisis pulmonali. Tuberculosis ordinarily happens in lungs, yet can additionally influence different parts of the body. It is spread through the air when individuals who have a dynamic TB infection cough, wheeze, or generally transmit respiratory liquids through the air. Most diseases don't have side effects, known as inert tuberculosis. Infections with advancement to active diseases, is one of the main cause for deaths and if left untreated, kills more than half of those so infected.

The side effects of dynamic tuberculosis incorporate interminable hack, fever, night sweats and weight reduction. The indications however differ as per the infected organ. The current routines for judgment incorporate radiological tests and microbiological society of body liquids and now and again biopsy. Finding of inactive tuberculosis depends on blood tests or tuberculin skin test. Notwithstanding, the medication incorporates a long time of chemotherapy which incorporates different anti-biotic over a long period of time. The significant problem circling the world however is, imperviousness to these anti-biotic and is prompting various resistant (MDR-TB) infections. Lungs are the most vulnerable organ for tuberculosis disease and nearly 90% cases are that of respiratory tuberculosis. Tuberculosis may turn into an endless sickness and reason far reaching scarring in the upper parts of the lungs. The upper lung projections are more influenced by tuberculosis than the lower ones (Golden and Vikram, 2005). The explanation behind this contrast is not so much clear.

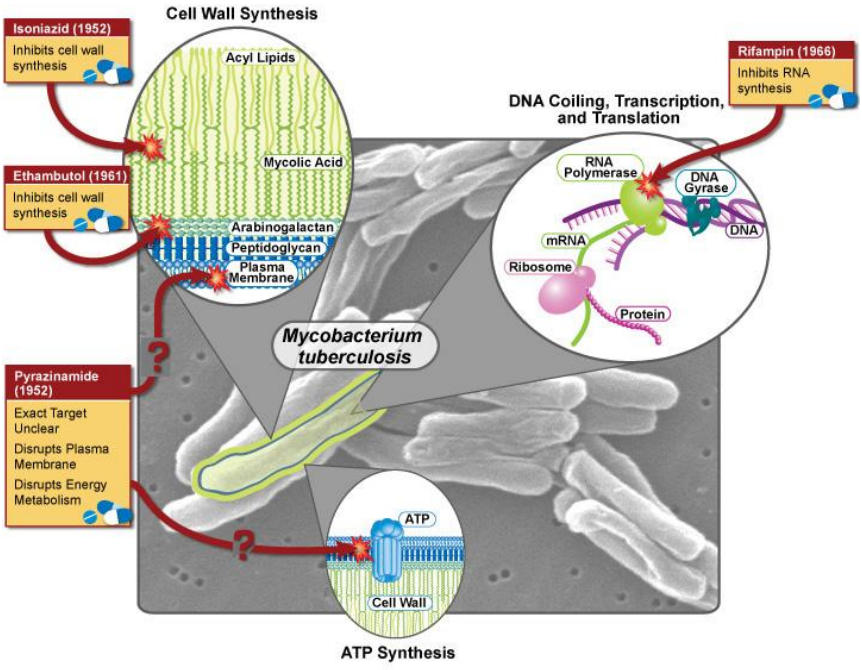

Figure 2: Drugs against *Mycobacterium tuberculosis*

On the other hand, in 15-20% cases the contamination crosses over to different organs. These contaminations happen either in adolescents or immunosupressed persons. Such cases are more common in HIV patients with around 50 % of them experiencing such diseases. Various elements make individuals more defenceless to TB contaminations. The most critical danger comprehensively is HIV; 13% of all individuals with TB are contaminated by this virus as well.

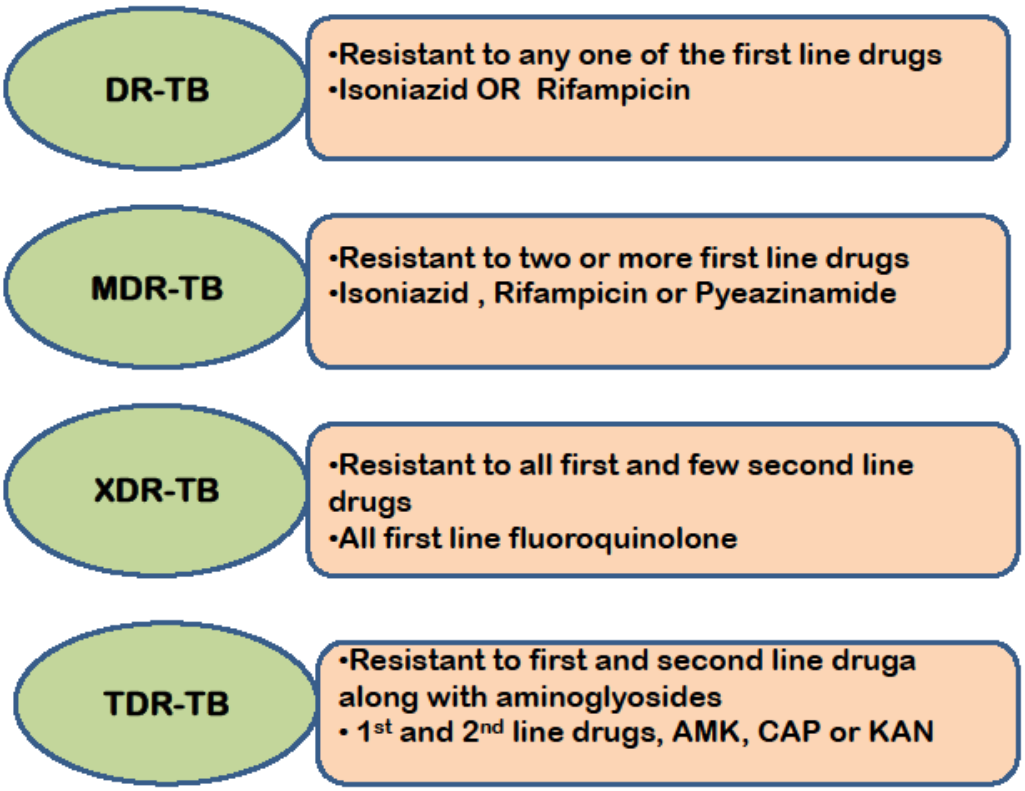

Figure 3: Classification of tuberculosis on the basis of resistance

Country	Population	Mortality	Prevalence	Incidence
India	1236687	170390	1900	2000
Africa	892529	160	2100	2100
America	961103	16	300	260
Global	7053684	790	11000	8300

Table 1: Estimated epidemiological burden of TB, 2012 (Numbers in thousands)

3.2 Understanding resistance mechanisms

The long term chemotherapy period coupled with improper drug use has prompted the development of drug resistant bacterial strains in the nature. From initially disengaged strains that were impervious to single medications, successive aggregation of safety transformations has prompted the rise of multidrug resistant (MDR), extremely drug resistant (XDR), and most as of late, total drug resistant (TDR) M. tuberculosis strains (Dorman and Chaisson, 2007; Ferrer et al., 2010). Accordingly, these resistant strains of M. tuberculosis represent a genuine risk to overall TB control programs. To handle the current scourge of medication resistant TB, novel helpful programs are desperately required. Other than endeavours to create totally new anti-biotics that are defined by the current safety systems, other non-conventional methodologies, for example, focusing on safety components or repurposing old medications need to be further examined. For these methodologies to be effective, drug safety systems in *M.tuberculosis* ought to be completely examined and well caught. Therefore, these resistant strains of *M. tuberculosis* pose a serious threat to worldwide TB control programs. Besides efforts to develop completely new antibiotics that are not affected by the existing resistance mechanisms, other non-traditional approaches such as targeting resistance mechanisms or repurposing old drugs need to be further investigated. For these approaches to be successful, drug resistance mechanisms in *M.tuberculosis* should be thoroughly studied and well understood.

3.2.1 Genetic mutation

The constantly expanding drug use because of escalating TB rates has brought about a relentless advancement of M. tuberculosis strains that are dynamically resistant to the accessible drugs. In light of this information, numerous current TB medications may well speak to this twofold edged sword. Both isoniazid and ethionamide require initiation by redox catalysts in the mycobacterial cytoplasm to get acitve. This methodology produces sensitive oxygen and/or radicals that push the mycobactericidal action (Ito et al., 1992; Wang et al., 1998). In any case once a mutant survives the killing activity of sensitive oxygen and radicals, these same compound matters would upgrade its impermanence prompting the obtaining of extra medication changes. Whether, and to what level, sensitive oxygen and radical species help the ascent of safety changes stays to be seen in M. tuberculosis (Smith et al., 2013).

Zhang et al. in 2013, found the emergence of multidrug-resistant (MDR) and extensively drug-resistant (XDR) tuberculosis has led to a fear of an epidemic. To understand the genetic mechanism Zhang et al., performed experiments on 161 clinical isolates. The work mainly focused on sequencing to identify resistance profiles led to significant progress in the area, discovering 72 new genes, 28 intergenic regions), 11 nonsynonymous SNPs and 10 IGR SNPs with strong, consistent associations with drug resistance. It was suggested that most of the resistance was conferred due to nonsynonymous mutations only (Zhang and Yew, 2009).

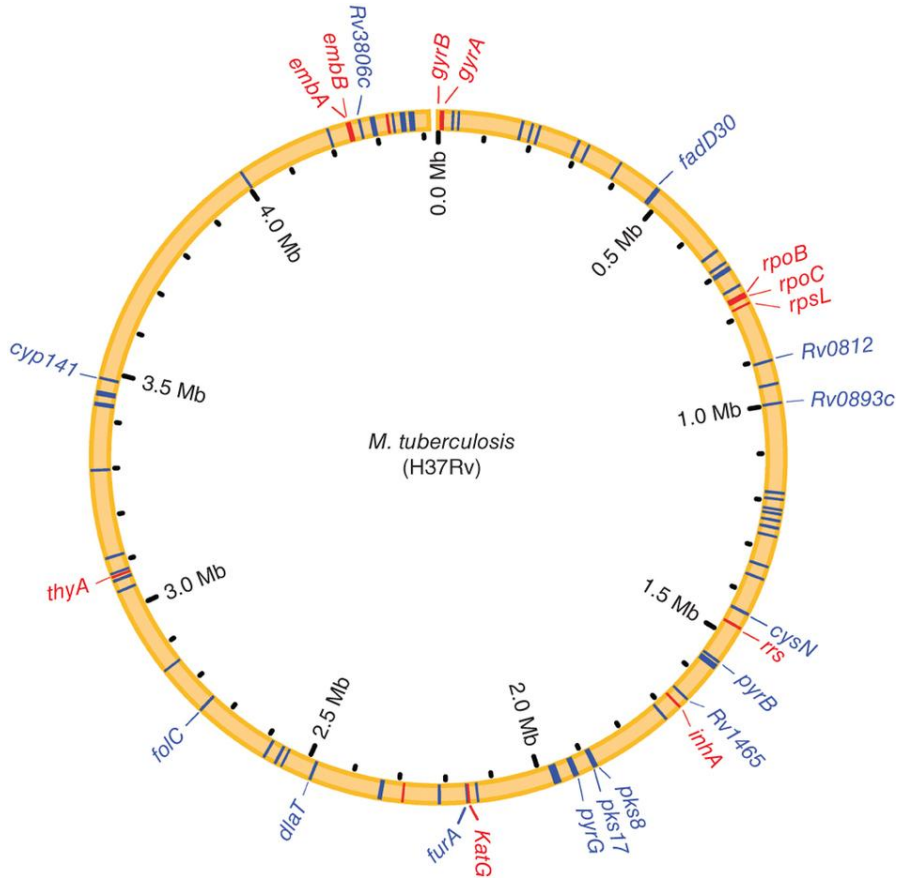

Figure 4: *M.tuberculosis* genome and genes associated with drug action

3.2.2 Modification of drug targets

Pathogenic bacteria have capability to surpass antibacterial activity of antibiotics by structural modifications in their targets, thereby hampering antibiotic binding affinity. The mechanism conferring resistance of *M.tuberculosis* to macrolide and lincosamide antibiotics serves as an example for this type of resistance. Mycobacterial species are by nature resistant to macrolides and lincosamides. These antibiotics inhibit the growth of bacterial cells by targeting protein machinery. They show reversible binding to a particular site in the 50S subunit of ribosome and thus inhibit peptidyl-tRNA to translocate (Buriankova et al., 2004). It was observed that the BCG (Bacillus of Calmette and Guérin) strain is unambiguously susceptible to macrolides and lincosamides while its parental *M. Bovis* strain remains resistant to the antibiotics. Later, through comparative genomics, it was realized that the sensitive BCG lacks a ribosomal RNA methyltransferase due to its chromosomal deletion of the *erm37* gene.

Direct chemical modifications are another method by which mycobacterium can inactivate antibiotics. Aminoglycosides are a group of antibiotics that constitutes an important position in the TB chemotherapy. These are broad range antibiotics and can have either bactericidal or bacteriostatic impact. Resistance to this class of compounds caused XDR-TB. Aminoglycosides can act differently in different conditions. Some act as protein biosynthesis inhibitors, although the mechanism remains unknown. Various studies in *M. smegmatis* and *M. Fortuitum* has led to identification of homologs of aminoglycoside 2'-N-acetyltransferase

(*aac*) that can confer resistance to gentamicin, dibekacin, tobramycin, and netilmicin. Homolog of AAC is has been indicated in *M. Tuberculosis* (Vetting et al., 2003) with its function in resistance being unknown. Surprisingly, the intrinsic resistance of *M. tuberculosis* to aminoglycosides has been attributed to the protein termed EIS (Enhanced Intracellular Survival) which was first discovered as a determinant of mycobacterial survival in host macrophages (Wei et al., 2000).

Drug	Mechanism of action	Gene involved	Function	Frequency of occurrence in mutants
Isoniazid	Inhibition of mycolic acid biosynthesis and other metabolic processes	KatG	Catalase-peroxidase	42-58
		InhA	Enoyl ACP reductase	21-34
		KasA	NADH dehydrogenase II	NA
		AhpC	Alkyl hydroperoxidase	10-15
Rifampicin	Inhibition of transcription	RpoB	β-subunit of RNA polymerase	96-100
Pyrazinamide	Inhibition of trans-translation	PncA	Pyrazinamidase	72-97
		FasA	S1 ribosomal protein	NA
Etambutol	Inhibition of arabinogalactan synthesis	EmbCAB	Arabinosyltransferases	47-65

Table 2: Mutations associated with drugs

3.3 Why target Pyrazinamide?

MDR TB or multi drug resistant tuberculosis is caused when resistance is developed for two or more 1st line drugs. Treatment of drug-resistant tuberculosis is hampered by poor efficacy and high toxicity of second-line drugs (Dooley et al., 2012). PZA is a pro-drug and acts only when metabolized by pyrazonic acid (POA). The enzyme pyrazonic acid is further derived from enzyme pyrazinamidase, encoded by *pncA* gene. Mycobacterial pyrazinamidase (MtPncA) is expressed in the cytoplasm and plays a pivotal role in the activation of pyrazinamide. This enzyme is expressed constitutively in the cytoplasm of M. Tuberculosis (Chang et al., 2011). Only after conversion of PZA into pyrazinoic acid by this enzyme the drug becomes potent. Destabilization of membrane potential and changes in the transport function are the underlying reasons for its bactericidal effect (Konno et al., 1967; Yeager et al., 1952; Zhang et al., 2008). Mutations in the *pncA* gene, which encodes a pyrazinamidase, is responsible for most of the pyrazinamide resistant *M. tuberculosis* strains (Scorpio and Zhang, 1996). Recently, few pyrazinamide resistant strains with mutations in the *rpsA* gene have also been identified (Shi et al., 2011).

The impact of resistance for drugs had been evident across the world lately. The problem is more profound in the case of Pyrazinamide drug due to issues pertaining to standardization of drug susceptibility testing. Next-Generation Sequencing for dentifying Pyrazinamide

Resistance in *Mycobacterium tuberculosis* was performed by Daum et al. in 2014. In order to perform NGS, 26 random samples of South African origin were selected which were diagnosed with either MDR or XDR TB. Nine out of 26 were found to be PZA resistant. The ratio 9:26 is an alarming ratio as PZA is one of the mojor drugs in the treatment. Using ion torrent method, the sequence of 9 patients was studied and it was observed that all of them contained one of the mutations conferring resistance. This methodology revealed the novel mutation lys-96-Arg.

3.4 Previous studies performed on PncA

Several variants of PncA protein have been identified which have been generated due to mutations in the gene. Studies have been performed to understand how these mutations leads to drug resistance against pyrazinamide. Major findings have been obtained from both *in silico* and wet lab studies.

Scorpio et al. in 1997 performed characterization of *pncA* mutations in pyrazinamide-resistant *Mycobacterium tuberculosis*. In order to understand PZA resistance on molecular level, authors cloned *pncA* gene and mutations in five PZA resistant strains were identified along with naturally resistant strains of *M. Bovis*. In this study, 38 PZA resistant clinical isolates and a few in vitro strains were analyzed. 33 out of 38 were found to possess *pncA* mutations and 8 in vitro samples were also found to contain these mutations. In order to identify the mutations PCR–single-strand conformation polymorphism (SSCP) technique was used. The identified mutations were dispersed along the *pncA* gene, but some degree of clustering of mutations was found at the following regions: Gly132-Thr142, Pro69-Leu85, and Ile5-Asp12.

Petrella et al., 2011 identified crystal Structure of the pyrazinamidase of *Mycobacterium tuberculosis.* A study was performed in wet lab to identify whether certain mutations cause resistance or not. Major mutations Asp8Glu, Lys96Gln, Ala134Val, Asp49Gly and Trp68Leu were considered for the study. For all the studied mutants total loss or very low residual levels of PZA activity was observed. Results from TSA assay depicted that there was a significant changes in the unfolding curves of the protein corresponding to the mutations Asp8Glu, Lys96Gln, Ala134Val, Asp49Gly and Trp68Leu, making them the most susceptible cause of resistance. Moreover, a significant decrease in the thermal stability of these mutants was also obtained. A decrease of 8 to 11uC in Tm was observed for Asp8Glu, Asp49Gly and Lys96Gln, thereby establishing the fact that these mutations have profound effect on the integrity of the 3D structure of PncA.

Sivashanmugam M, 2013, studied the mechanism of resistance of novel mutation Ala-102-Pro. This mutation was found to have no effect on the conformation of the protein. However the inhibitory constant was higher than that of the wild type. The study shows that resistance was due to change in the interaction patterns between the ligand and protein. The mutant protein was found to be less stable than the wild. However, Ala102 in WT was found to be

less fluctuating and more stable in molecular dynamics simulation when compared to Pro102 in MT which was highly fluctuating and unstable. This implies that Ala102 shall be a key residue involved in PZA inhibitory interactions. Moreover, MT does not show hydrogen bonding with PZA with Pro102 and also deviating in terms of PZA binding pose in comparison with WT. Hence, the observed deviations in terms of MT-PZA interactions shall be attributed to the drug resistance conferred.

Sethumadhavan, 2014, studied drug resistance mechanism of PncA in *Mycobacterium tuberculosis*. In their study three mutations D8G, S104R and C138Y of PncA which are involved in resistance towards PZA were considered. Studies including binding pocket analysis, solvent accessibility analysis, docking studies, analysis of ligand-protein interactions and molecular dynamics studies were performed to understand the mechanism. They identified that these mutations led to rigidness of the cavity making it difficult for the drug to bind properly with the active residues. The mutations supposedly led to contraction of the active site which was confirmed by analysing the RMSD and radius of gyration coupled with Principal component analysis and Euclidean distances.

3.5 The Protein PncA

PncA protein is involved in the activation of the pyrazinamide drug by converting it to pyrazonic acid. Pyrazinamide is a first line drug and an extremely effective therapy against tuberculosis. The crystal structure of PncA was determined in 2011 by and has been submitted in the PDB. The sequence of PncA bears similarity with *Pyococcus horikoshii* and *Cinetobacter baumanii*. The 3-D structure however shows decent dissimilarities. In M. tuberculosis, this active site reigion was found to contain a Fe2+ ion surrounded by one aspartate and three histidines. The binding cavity is formed by Cys138-Asp8-Lys96 motif showing the essence of a cysteine-based catalytic mechanism (Petrella et al., 2011).

3.5.1 Crystal structure of the *M. tuberculosis* PncA protein

The crystalline structure of PncA was detrmined to 2.2Å. The structure was obtained by rreplacing residues in PhPncA. The final structure consists of 185 residues. The structure of PncA is made of a six-stranded parallel betasheet and four alpha helices. The helices are packed on both sides of the beta sheets to form an a/b single domain (Figure 5). The active site cysteine residue Cys138 is present in Helix a3. Fe2+ is also present in PncA. The iron atom confers a distorted tetragonal bipyramidal arrangement rendered by the side chains of residues His51, His71 and two water molecules, HOH220 and 221 and the side chains of Asp49 and His57 (Figure 5) (Petrella et al., 2011).

3.5.2 Description of the *M. tuberculosis* PncA active site

The active cavity in MtPncA is a small cleft, approximately 10 A ° deep and 7 A ° wide.The active cleft contains residues Lys96 at the end of strand b3, Asp8 at the end of strand b1 and Cys138 at the N-terminal. Opposite of the active site lay 3 His residues His51, His57 and His71 which along with Asp49, hold the Fe ion. Another important region in the protein is

from residues 50-72. This forms the loop in the protein which acts as the lid of the binding site. In the most bulged out region of this loop, Trp68, is present above the catalytic cleft such that, with His137 and Phe13 it defines the boundary of the cavity. Lastly, one more a significant characteristic of the active site of PncA is the formation of a cis-peptide bond between residues Ile133 and Ala134, thereby orienting the amide nitrogen atom of Ala134 toward the active site centre. This is the reason that it can form an oxyanionhole with the amide nitrogen of Cys138 (Figure 6) (Petrella et al., 2011).

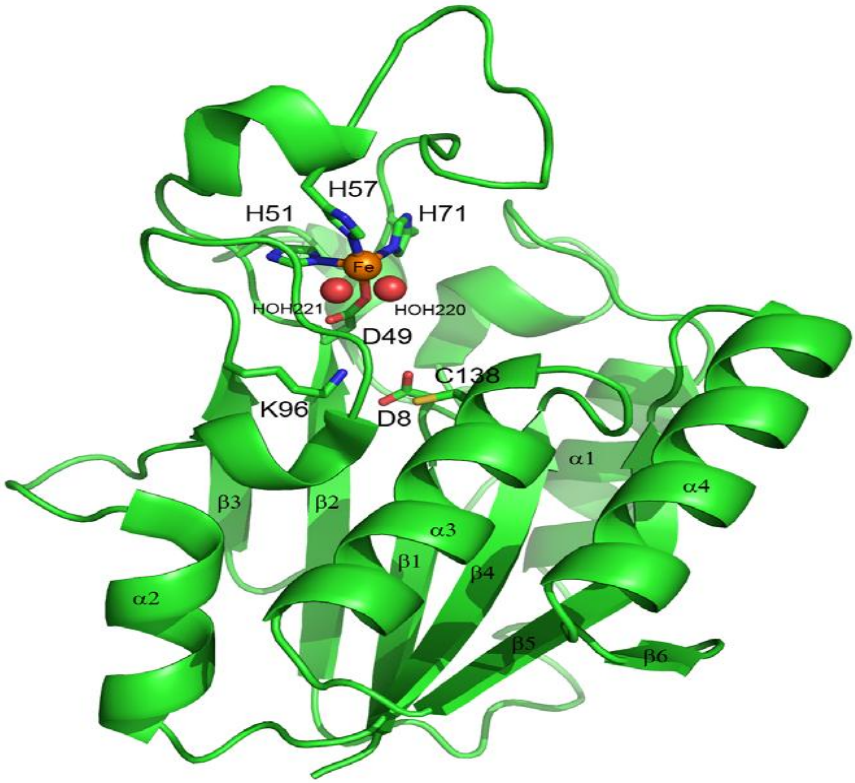

Figure 5: Ribbon representation of the structure of the M. tuberculosis PncA protein

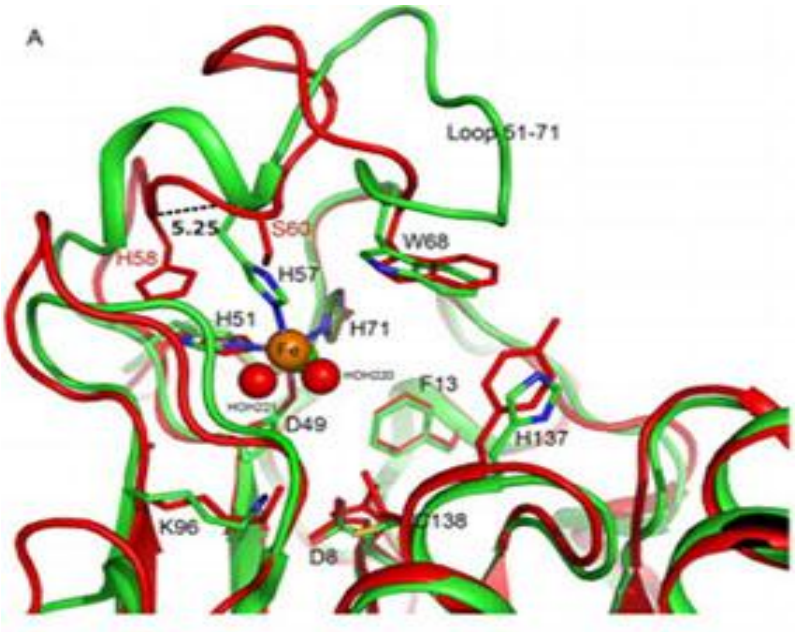

Figure 6: Detailed description of the active site region in MtPncA.

3.6 Recent developments and advancements

The current chemotherapy regime against tuberculosis was developed between 1940's and the 1980's. There has been a prolonged silence in this field which led led to escalation in HIV positive cases and DR-TB (drug resistant-TB). The new therapeutic research is focused on shortening of chemotherapy period for improvement in DR-TB treatment and making a TB-HIV combined therapy available. For this purpose, several new drugs are under clinical trials and other strategies for faster and efficient development have surfaced in recent years.

Diarylquinolines selectively inhibt mycobacterial ATP synthase and show minimal activity against other bacteria or eukaryotic cells (Andries et al., 2005). Bedaquiline, the first drug in the class (previously known as R207910 and TMC-207), was discovered by screening of compounds against *M smegmatis*. It has proved to be bactericidal against rapidly growing resistant organisms and is effective against DS and DR-TB (Andries et al., 2005; Koul et al., 2008; Rao et al., 2008). In view of the urgent need for new therapeutic agents, the US Food and Drug Administration has accelerated approval and licensing of bedaquiline for use in MDR-TB in 2012. In humans, a Phase IIa EBA trial has shown that a daily dose of 400-800mg had equivalent efficacy to isoniazid and rifampicin after 5^{th} day (Rustomjee et al., 2008).

From each of the drug classes described above, atleast one of them is being examined in Phase III trials. However, several other compounds at earlier stages of development are also there. The oxazolidinones possess broad spectrum antimicrobial activity. They bind to the 70S initiation complex of bacterial ribosomes and interfere with protein synthesis. Linezolid, the only currently licensed drug in this class has displayed activity against *M. tuberculosis*

(Dietze et al., 2008) and it has been used without label in combination therapy for MDR-TB.Many more oxazolidinones are under development which includes sutezolid (PNU-100480) and posizolid (AZD5847) (Shaw and Barbachyn, 2011). Hopes are high that these will show improved sterilising activity and lower toxicity.

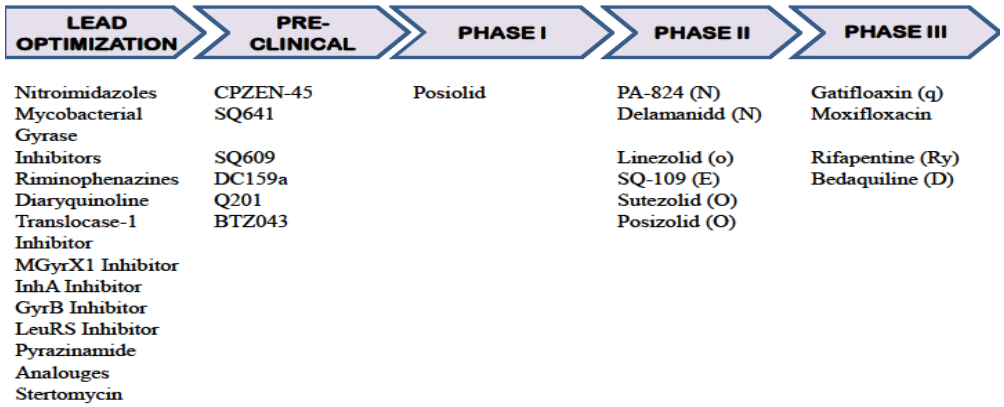

. :

Figure 7: Summary of Recent Developments

3.7 Modification of existing drugs

As a new strategy for drug discovery and development focus has shifted on drug re-profiling as a way to identify new treatments for diseases. In this strategy, the actions of existing medicines, whose safety and pharmacokinetic effects in humans have already been confirmed clinically and approved for use, are examined comprehensively at the molecular level and the results used for the development of new medicines. This strategy is based on the fact that we still do not understand the underlying mechanisms of action of many existing medicines, and as such the cellular responses that give rise to their main effects and side effects are yet to be elucidated. To this extent, identification of the mechanisms underlying the side effects of medicines offers a means for us to develop safer drugs. The results can also be used for developing existing drugs for use as medicines for the treatment of other diseases. Promoting this research strategy could provide breakthroughs in drug discovery and development.

METHODOLOGY

Data set

In order to perform the analysis, 3-D structure of protein was required. We selected native PncA (PDB ID 3PL1) structure from Protein Data Bank (PDB) (Berman et al., 2002; Petrella et al., 2011). The pdb structure contains a Fe2+ ion, surrounded by one aspartate and three histidines in the substrate binding cavity and three water molecules. The active site is formed by three residues Asp8, Lys96 and Asp138 (Rajendran and Sethumadhavan, 2014). Since the mutant structure of the protein was not available in the database, the mutation was induced *in silico*. The 3-D structure of the drug molecule PZA was taken from drug bank in .sdf format for our investigation (Wishart et al., 2008).

Optimization of protein and ligand

The protein crystal structure of PncA was obtained from Protein Data Bank [PDB ID: 3PLI]. However the protein contains three crystallized water molecules. In order to perform further analysis the crystallized water molecules were removed using Accelyrs Viewerlite 5.0.

Since the mutant structure was not available in the database, a point mutation was induced at 96^{th} position in the native structure using maestro, a Schrodinger product, to create a mutant protein. The position was selected from the sequence window and the 96^{th} lysine residue was mutated to arginine. The orientation of the protein and ligand were optimized before further analysis. The protein with removed water crystals was further prepared using Schrodinger's protein preparation wizard (Madhavi Sastry et al., 2013; Schrödinger Release 2013-1: Schrödinger Suite 2013 Protein Preparation Wizard; Epik version 2.4). In this process hydrogen were added, bond lengths were optimized, disulfide bonds were created, terminal residues were capped and selenomethionines were converted to methionine. The ligand molecule obtained from the drug bank was also prepared using LigPrep (Schrödinger Release 2013-1: LigPrep). The tool generates all possible chiral, stereochemical and ionization variants of the ligand.

Binding cavity analysis

The size of the binding cavities is an important measure in mutational studies. To compare the binding cavities of native and mutant proteins, we have used CASTp server. Weighted Delaunay triangulation and the alpha complex are used for shape measurements in CASTp. Information on surface accessible pockets and interior inaccessible cavities of a protein is generated by the server. The volume and area of each pocket and cavity in solvent accessible surface (SA, Richards' surface) and molecular surface (MS, Connolly's surface) are calculated. Number, area and circumference of mouth pockets are also calculated. CASTp algorithm is based upon recent developments in Computational Geometry. It has certain advantages: 1) analytical identification of pockets and, 2) precisely defined boundary

between solvent and pocket 3) calculated parameters does not make use of dot surface or grid points and are rotationally invariant (Joe Dundas, 2006).

The protein .pdb structures are submitted and results are displayed in Jmol and interface is user friendly and results can be analyzed interactively. All the default values are used. The default value of 1.4Å for probe radius is used.

Protein ligand interaction

Receptor–ligand interaction analysis was performed for native and mutant PncA with PZA. In order to carry out the docking simulation, we used the Glide module of Schrodinger as molecular-docking tool (Friesner et al., 2004; Small-Molecule Drug Discovery Suite 2013-1: Glide). In this docking analysis, flexible docking protocols were used and both protein and ligand were kept flexible.

Proteins were prepared using Potein Preperation Wizard tool in Glide. Atom charges were assigned and polar hydrogens and were added into the protein PDB file for the preparation of protein for docking. Ligands were prepared using ligprep. In order to perform docking, a grid was created around the active site of the protein molecule using Glide module of Schrodinger. The grid was generated around Asp8, Phe13, Asp49, His51, His57, Phe58, Gly60, Trp68, His71, Lys96, Ile133, Ala134, Thr135, and Cys138. The grid confines the site of the protein where the software would induce docking with the ligand. Extra precision docking was then performed for native and mutant proteins with PZA.

Total ligand–receptor interaction energy along with its components like van der waals energy, electrostatic energy etc are also calculated. The electrostatic energy gives a measure of how a molecule interacts with another nearby molecule. The two molecules interact with each other through their mutual electrostatic interactions. The electrostatic energy being the only long-range non-bonded interaction, its value is calculated for two atoms that are separated by three or more bonds. The negative value of electrostatic energy indicates better interaction and vice versa. Since hydrogen bonds and van der Waals contacts consists complementary surfaces, these surfaces must be able to pack closely together, creating many contact points allowing charged atoms to make electrostatic bonds. Thus, polar interactions and van der waals contribute to the dynamic stability of the ligand–receptor complex (Jones and Thornton, 1996).

Molecular dynamics simulations of the docked complexes

In order to investigate the mechanism of resistance in the docked complexes, molecular dynamic study was performed in the presence of an explicit solvent on a fully hydrated model using explicit triclinic boundary with harmonic restraints. The simulations were performed using Desmond Molecular Dynamics module of Schrodinger, with Optimized Potentials for Liquid Simulations (OPLS) all-atom force field 2005 (Schrödinger Release 2013-1: Desmond

Molecular Dynamics System; Shivakumar et al., 2010). The complexes were prepared before simulation by addition of hydrogen followed by optimization, removal of water molecules, capping of end terminals and generation of disulphide bonds using the protein preparation wizard. First step in molecular dynamics is solvation of protein complex. Prepared protein-ligand complexes were then solvated with SPC water model in a triclinic periodic boundary box. To prevent interaction of the protein complex with its own periodic image, the distance between the complex and the box wall was kept 10 Å. Energy of the prepared systems was minimized to 5000 steps using steepest descent method or until a gradient threshold of 25kcal/mol/Å was achieved. It was followed by L-BFGS (Low-memory Broyden- Fletcher-Goldfarb Shanno quasi-Newtonian minimiser) until a convergence threshold of 1 kcal/mol/Å was met. For system equilibration, the default parameters in Desmond were applied. The equilibrated systems were then used for simulations at a temperature of 300 K and a constant pressure of 1atm, with a time step of 2fs. For handling long range electrostatic interactions Smooth Particle Mesh Ewald method was used whereas Cutoff method was selected to define the short range electrostatic interactions. A cut-off of 9 Å radius was used. The protein complexes were then simulated for 15 nanoseconds.

Combinatorial library generation

After analysisng the mechanism of resistance, next step was to develop derivatives of pyrazinamide which could be used as new drug leads and could bind to both wild and mutant PncA. In order to do so leadgrow module of vlife MDS was used. The tool allows creating a library of compounds based on a common template. The template should contain substitution sites, the tool then applies permutation and combination to create a vast library of compounds. The greater the number of substitution sites, bigger is the library. 2 different libraries were created based on two templates. One template was original PZA with $–NH_2$ and =O replaced by other groups. This template consisted of 4 substitution site. The second template was formed from the 5-chloropyrazine-2-carbonyl chloride, which is formed by combination of two different PZA derivatives. These compounds have shown to be possess efficient anti-bacterial effect in studies performed . The template consisted six substitution sites. In order to generate the library, leadgrow was selected from the module dropdown of Vlife MDS. The template was introduced in the tool along with the substitution sites. Select the substitutions that are to be made in the template. The tool then generates all possible combinations and the compounds are saved in .mol2 format.

RESULTS

Continuous emergence of new mutations associated with drug resistance in *M.tuberculosis* is posing a great danger to the conventional therapies. The methods need to be revised according to the current situation which requires generous understanding of the mechanisms of resistance. In order to identify one such mechanism we have tried to analyse the mutation K96R occurring in the active site of *M.tuberculosis*. Several analyses have been made in order to understand the mechanism at atomic level.

Binding cavity analysis

Binding pocket analysis is an important measure to identify the impact of mutation on the cavity. The pocket volume for both native and wild were calculated using CASTp server. The structures obtained after molecular dynamics were used for the calculation of the pocket volume. The volume of the cavity for native protein PncA was 551.9 $Å^3$ and that of wild was 1314.2 $Å^3$. A considerable difference can be seen in the two volumes (Figure 8). The increase in cavity volume affects the stability of ligand and, in turn, affects the ligand–receptor. In order to evaluate further the behaviour of the mutant, we performed docking and molecular dynamics studies.

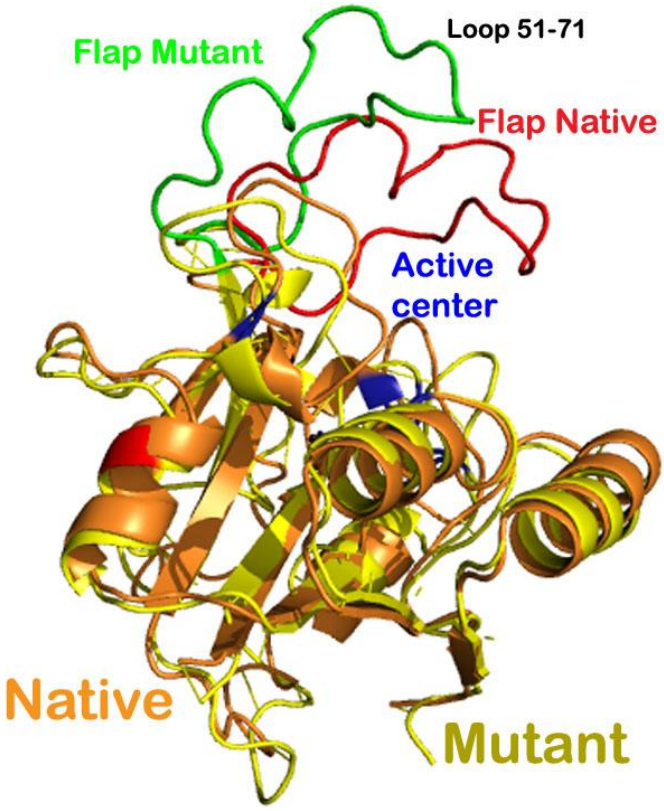

Figure 8: Ribbon representation of the alignment of structures of the native and mutant *M.tuberculosis* PncA protein

Interaction analysis between receptor and ligand molecule

Interaction energy calculation is one of the most significant parameters to understand the biological activity of ligand protein complex. Previous studies on PncA have shown the significance of vander waal interactions. Binding energy calculations provide information on both vander waal and electrostatic energy of the complex.

The value of van der waal's energy and electrostatic energy for native complex was calculated using Glide and was found to be -17.16 kcal/mol and -10.27 kcal/mol respectively. The glide energy or the total ligand-receptor energy was found to be -27.43 kcal/mol for the native complex. On the contrary, there was a significant difference in the values for mutant complex. The values for van der waal energy, electrostatic enrgy and glide energy were -10.86, -13 and -23.43 kcal/mol respectively (Table 3). Hydrogen and hydrophobic interactions are the most significant interactions in the binding. The interaction plots were generated using ligplot.

Protein	Docking Score (Kcal/mol)	Glide Energy (Kcal/mol)	Electrostatic energy (Kcal/mol)	Vander waal Energy (Kcal/mol)
Native	-4.025	-27.43	-17.16	-17.16
Mutant	-3.77	-23.434	-13.0	-10.86

Table 3: Docking results of wild and mutant PncA with PZA

In native complex, the oxygen of PZA was found to be making one hydrogen bond with nitrogen of 134Ala of PncA and the distance was 3.19Å (Figure 9). The ligand also made a significant number of hydrophobic bonds with Asp 8, Phe 13, leu1 9, Val 21, Ile 133, His 137, Cys 138 and Val 163 of PncA (Figure 10). On, the other hand the mutant protein was found to be making two hydrogen bonds. The oxygen of the ligand was making hydrogen bonds with nitrogen of Ala 134 and Cys 138 of mutated protein and the bond lengths were 3.11Å and 3.08Å respectively (Figure 11). However, the number of hydrogen bonds was reduced to four as compared to native complex which made eight hydrophobic bonds. Ligand made hydrophobic bonds with Asp 8, Gln 10, Ile 133, His 137 of mutant protein (Figure 12). We observed a remarkable difference in the interactions in the two proteins. Cys 138, one of the key residues is involved in hydrophobic interactions in native complex while in mutant complex; it is forming a hydrogen bond with the ligand. In above analysis, mutants showed less ligand interaction and docking score compared to native enzyme which inspired us to investigate the structural arrangement of biding residues in 3D space.

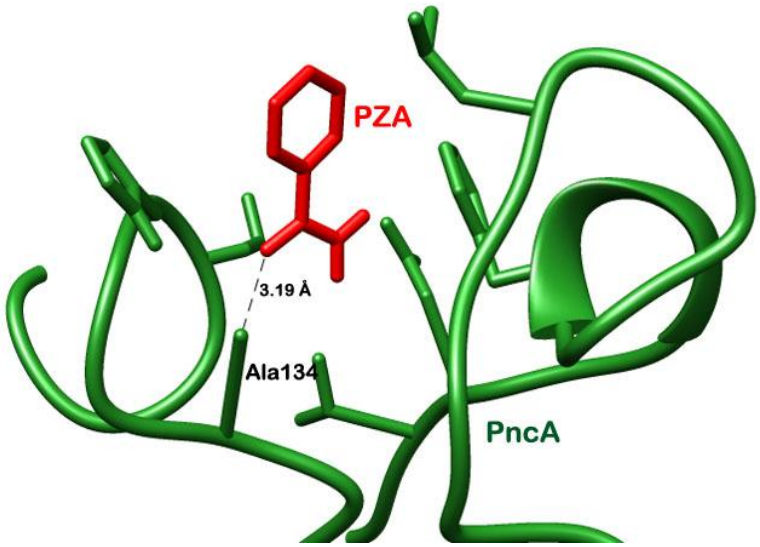

Figure 9: Hydrogen bond interactions of native PncA with PZA

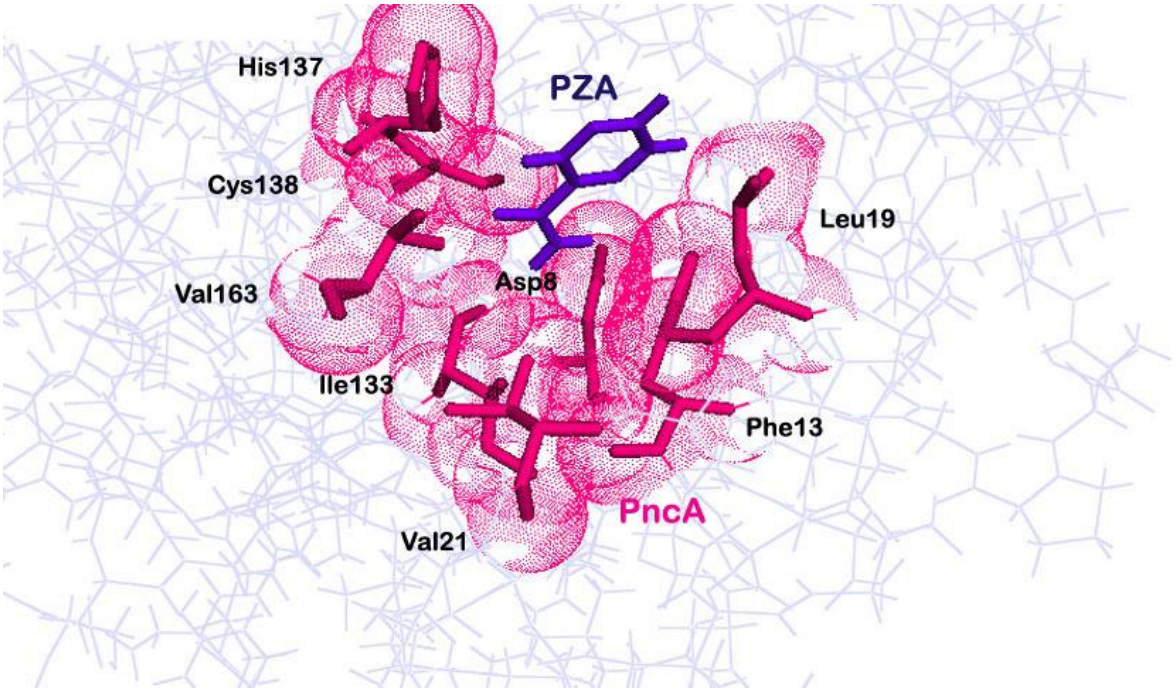

Figure 10: Hydrophobic interactions of native PncA with PZA

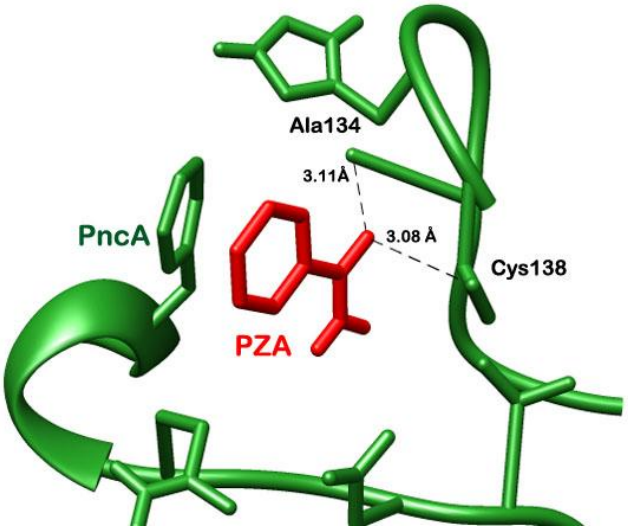

Figure 11: Hydrogen bond interactions of mutant PncA with PZA

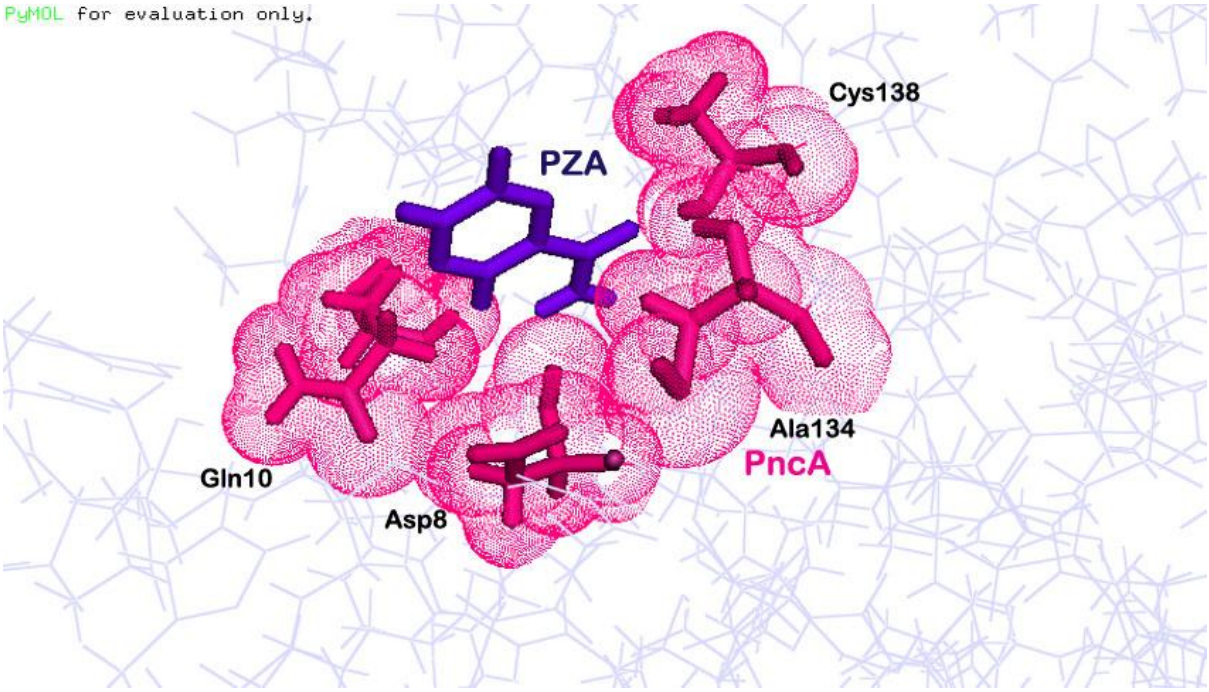

Figure 12: Hydrophobic interactions of mutant PncA with PZA

The three factors typically used to judge the resistance level, namely, volume of binding pocket, docking score and interaction energy, all supported the weak binding of the ligand with protein thereby hampering its activation. However, increased number of hydrogen bonds in mutant complex was suspicious. Therefore, in order to study the conformational changes of the complexes in *in vivo* conditions, we performed molecular dynamics studies. RMSD, Rg, RMSF were investigated to understand the behaviour of binding between ligand and enzyme.

Investigation of flexibility of native and mutant PncA enzyme

In order to get conformational fluctuations, MD simulations were performed for native and mutant PncA. Since, the structure of mutant protein was not available in the data-base; we had artificially induced mutation in the protein. Thus, in order to bring about the mutant protein in a stable conformation, MD simulation was performed on the mutant protein. The simulation was performed for 15 ns. The protein was initially unstable and RMSD was continuously increasing up till 6 ns after which it became stable at 4Å with a few minor fluctuations (Figure 13).

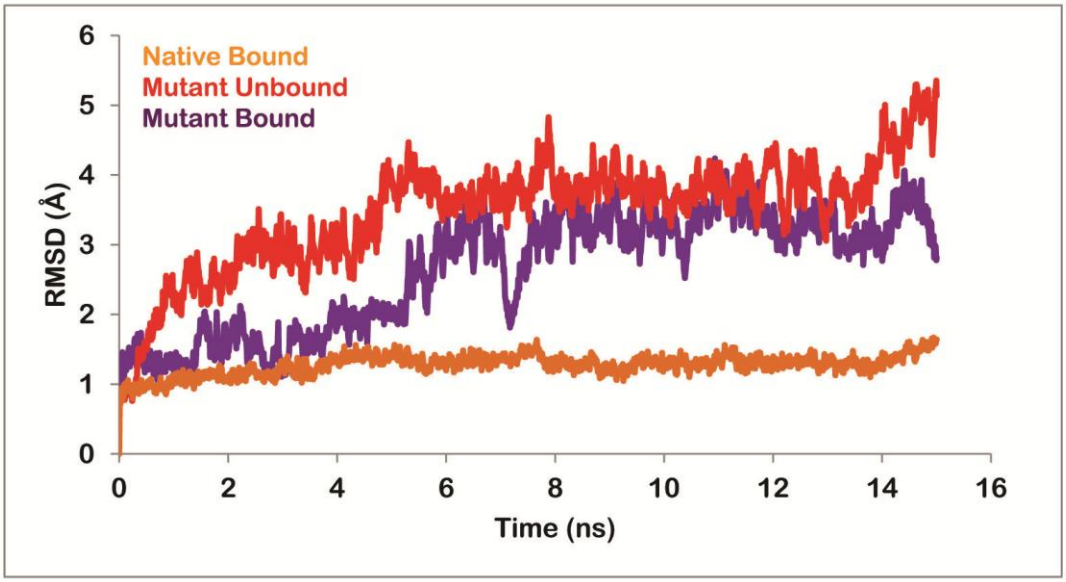

Figure 13: RMSD plots for mutant unbound, native bound and mutant bound complexes

For protein complexes, RMSD was calculated for all the atoms of the native structure, which was considered to identify the convergence of the mutant structures. The native complex structure showed fluctuation till 2 ns, after which it got stabilized at 1.3Å till 8ns. Sudden

fluctuations were observed at 9 ns and RMSD went up to 2Å. The protein complex again became stable after that up to 15ns at 1.5 Å RMSD. However, in the mutant structure, the protein complex stabilized from 2ns to 5ns at 3Å and sudden fluctuations were observed at 6ns. The plot however was stable beyond 6ns to 15ns between 3-4Å. The RMSD analysis depicts that native structure showed more fluctuations but in a small range. However, in mutant protein, RMSD went up initially but the protein got stabilized with fluctuations not more than 1 Å (Figure 13).

Major influence in the interaction pattern of the native and mutant complexes was observed after molecular dynamics studies. In native complex, the number of hydrogen bonds increased to two. The oxygen of ligand was making two hydrogen bonds with nitrogen of Ala 134 and Cys 138 with bond lengths 3.33Å and 2.89Å respectively (Figure 14). The hydrophobic bonds however reduced from eight to five. The ligand was now making hydrophobic bonds with Asp 8, Phe 13, Val 21, Ile 133 and His 137 (Figure 15). On the other hand, mutant complex was now making only one hydrogen bond with Ala 134 (Figure 16) and seven hydrogen bonds with Asp 8, Gln 10, Phe 13, Asp 49, Ile 133, His 137 and Cys 138 (Figure 17). The bond length for the corresponding hydrogen bond was observed as 3.06Å.

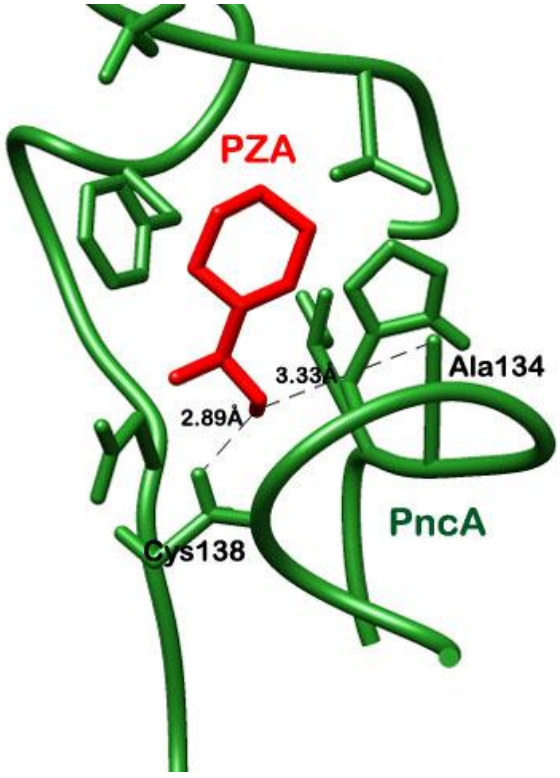

Figure 14: Hydrogen bond interactions of native PncA with PZA after Simulations

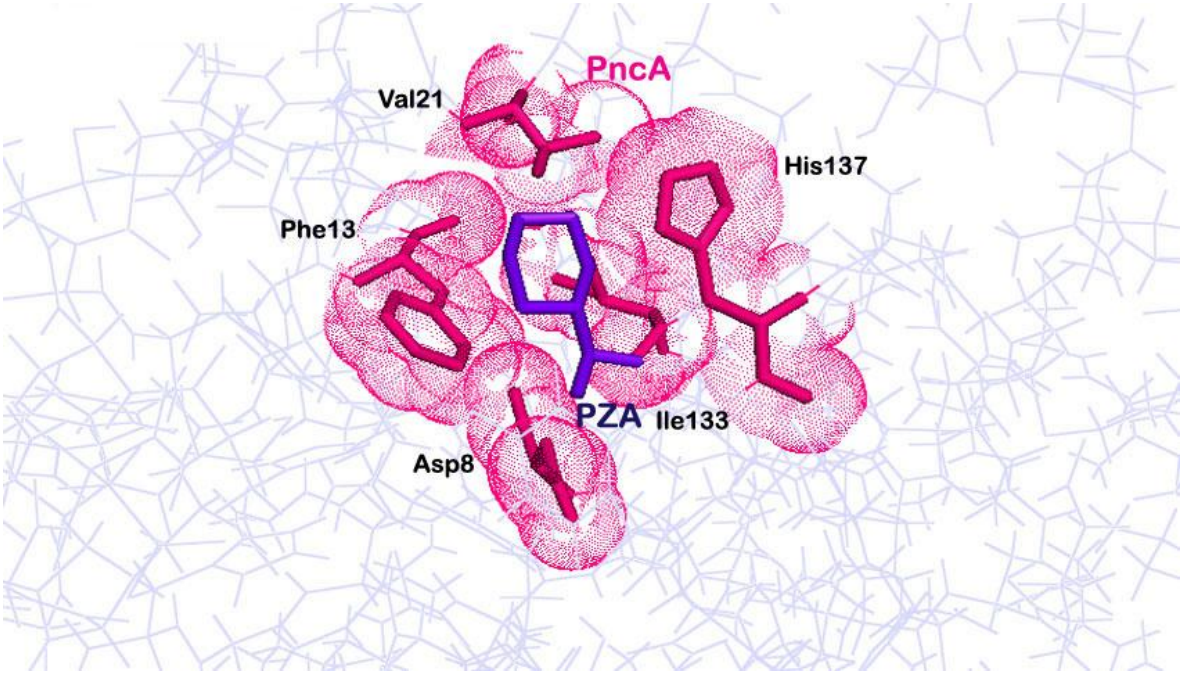

Figure 15: Hydrophobic interactions of native PncA with PZA after Simulations

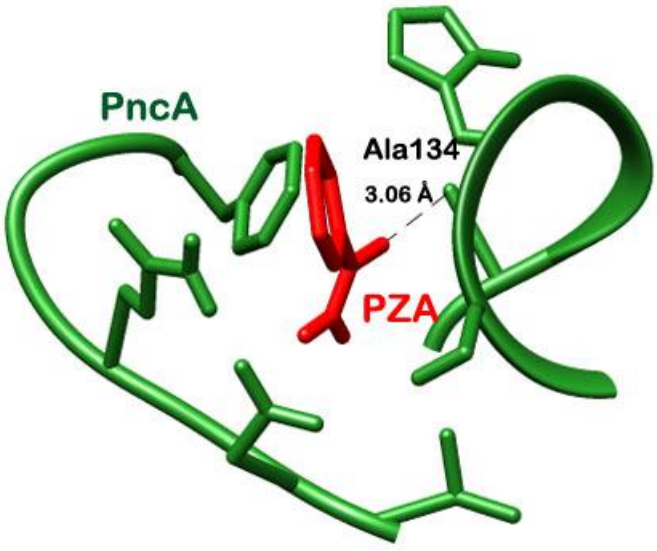

Figure 16: Hydrogen bond interactions of mutant PncA with PZA after Simulations

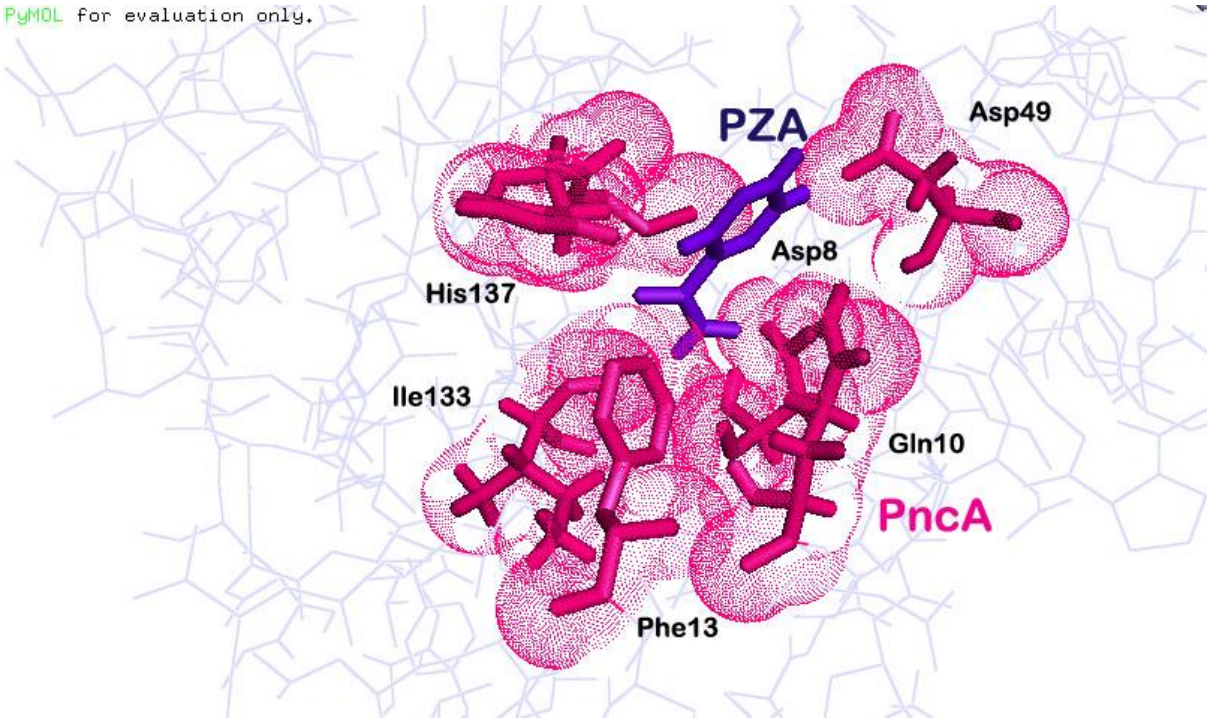

Figure 17: Hydrophobic interactions of mutant PncA with PZA after Simulations

The radius of gyration is defined as the mass-weighted root mean-square distance of a cluster of atoms from their common canter of mass. In other words, the radius of gyration of a protein is a measure of its compactness. A protein will maintain a steady value of R_g if it is stably folded, and the value will fluctuate if the protein unfolds. The radius of gyration was plotted against time and the data was analysed. The native complex curve is stable throughout the simulation period and fluctuations are very low. This low value of fluctuations can be attributed to high stability and compactness of the protein. The mutant protein complex curve is however more fluctuating and the value for R_g are as high as 17 Å (Figure 18). The fluctuations are prevalent during entire simulation period and from this it can be inferred that unfolding of protein is taking place. The fluctuations are highest in the loop region as can be seen in RMSF plot (Figure 19). From data visualization we can say that unfolding might be occurring at this loop region and can be seen clearly in Figure 19. The loosening of the loop region therefore affects the binding of the residues.

To determine the affect of mutation on the residues, RMSF values of whole complex was calculated for both native and mutant bound and unbound complexes. Analysis of the data revealed high level of fluctuations in the mutant complex compared to native. The fluctuations were widespread in the entire mutant protein, while in native sequence small fluctuations were observed in certain regions. The fluctuations in certain residues in native protein confer flexibility to the protein and keeping it compact at the same time. While in case of mutant protein, high level of fluctuations results in high mobility in the residues resulting in a loosely packed protein. The RMSF of binding residues, i.e. Asp8, Phe13, IIe133, Ala134 and Cys138 of native and mutant structures were also analysed. The fluctuation of binding residues was very small in case of native protein and the values were between 0.4 to 0.9 Å. In case of

mutant protein the RMSF of these residues was intermediate in both unbound and bound mutant protein structures (Table 4).

Protein	Asp8	Phe13	Ile133	Ala134	Cys138
Native Bound	0.635117	0.572594	0.496256	0.5135	0.476051
Mutant Unound	0.890527	1.71058	0.84011	0.91584	0.731542
Mutant Bound	0.795579	0.948946	0.858351	0.99094	0.988013

Table 4: RMSF values of binding cavity residues in nm

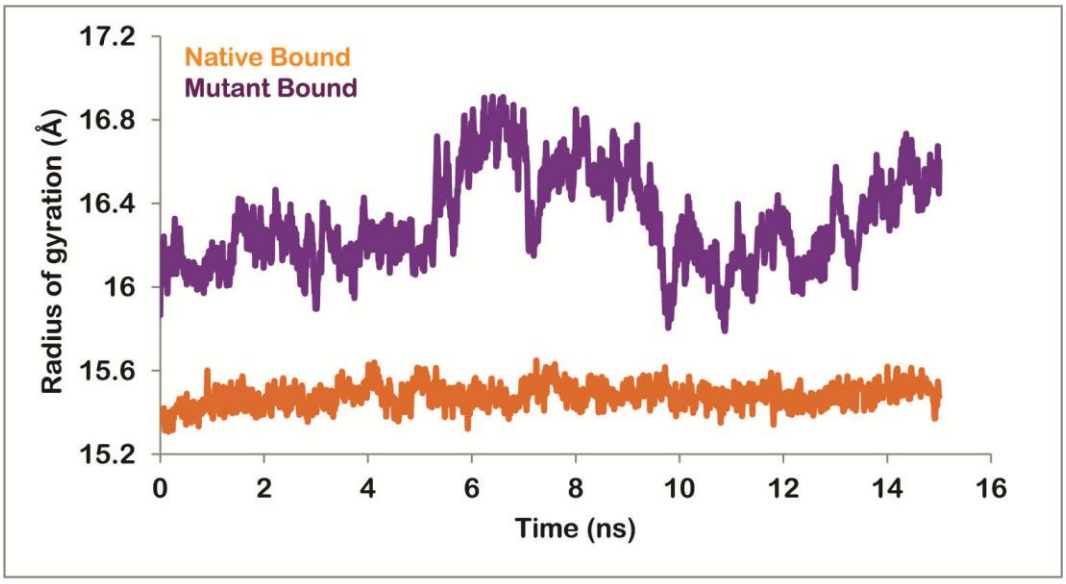

Figure 18: Radius of gyration for native bound and mutant bound

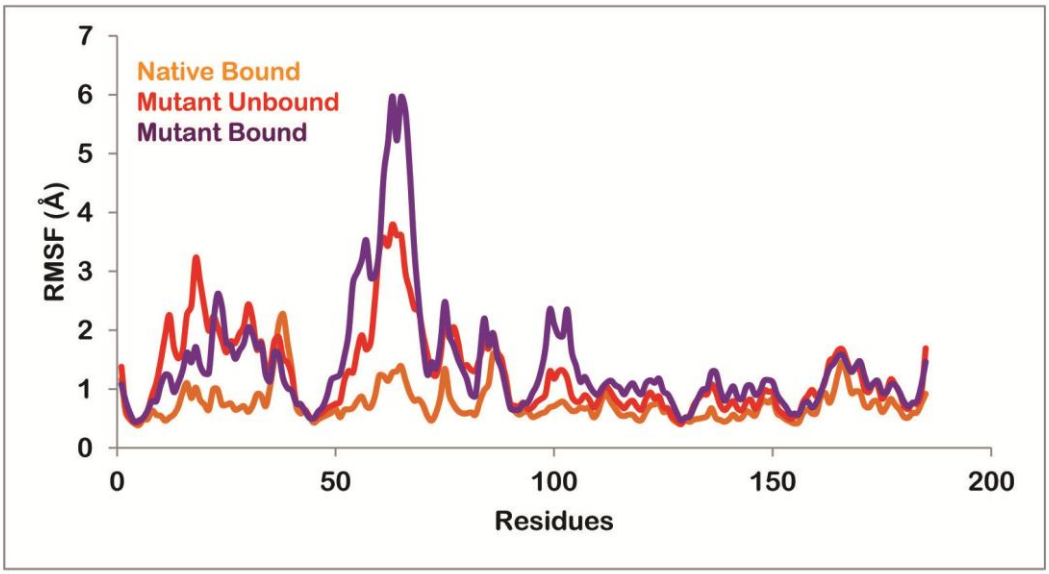

Figure 19: RMSF values for native bound, mutant unbound and mutant bound protein complexes

Comparison of bound and unbound native and mutant protein was also performed to analyse the behaviour of important residues post binding. The highest fluctuation in unbound mutant was 3.79 Å and in case of mutant protein-ligand complex the highest fluctuation was 5.97 Å. According to a study, residues 50 to 70 compose an important loop region which is involved in holding the ligand in position after binding. An important inference can be made from the RMSF values of these residues. In case of native bound protein the fluctuations were found to be in the range 0.5 to 1.7 Å. However in case of mutant unbound, the RMSF in these residues indicates flexibility which is important for ligand binding. The values were in the range 0.5-4 Å. After binding these fluctuations should be low like in case of native bound protein. However, the trend was opposite in case of mutant complex. The fluctuations were higher in the loop region in mutant complex and were in the range 0.5-6Å which is quite high. These high fluctuations results in highly mobile loop region and thus cannot hold ligand in place (Figure 19).

Combinatorial library analysis

Our aim was to identify new derivatives of PZA which could be more efficient against resistant strains. For this purpose, two combinatorial libraries were generated based on two different templates using LeadGrow tool of Vlife MDS. The substitution was made by different alkanes, atoms, aromatic compounds and rings. First library consisted of 60,000 componds and second library had more than 1,50,000 compounds. The prepared dataset of about 0.2 million natural compounds was docked with the crystal structure of PncA, both

wild and mutant, to screen compounds with high binding affinity. A total of 423 compounds with glide score more than -5 (in magnitude) were screened and subjected to extra precision (XP) docking protocol of glide. The top scoring compound was selected on the basis of Glide Score and Emodel score (Table 5). Emodel score is used to select the top ranked pose of each ligand and present it to the user. The compound, *N-phenylpyrazine-2-carboxamide*, possessed the highest glide XP score of -8.183 Kcal/mol and Emodel score of -105.435 Kcal/mol when docked with wild PncA and XP score of -7.681 Kcal/mol and Emodel score of -100.76 Kcal/mol when docked with mutant PncA. For our convinience we will use the name PPC (Figure 20).

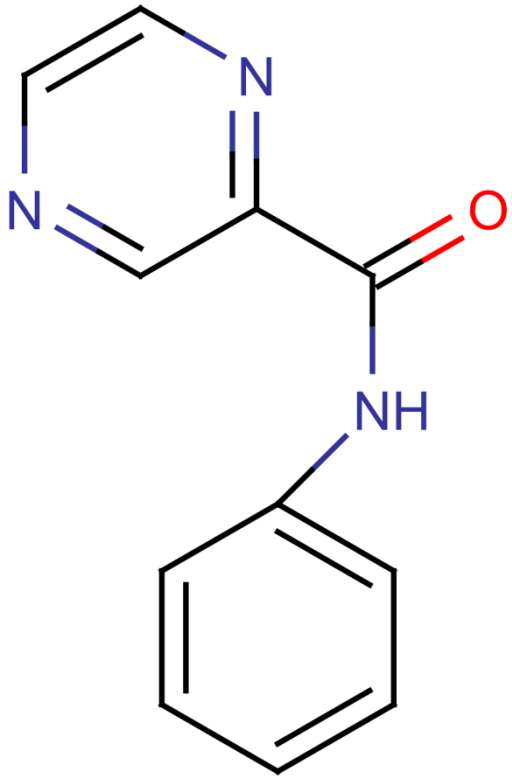

Figure 20: N-phenylpyrazine-2-carboxamide

Analysis of the components of Glide score revealed that van der Waals energy (E_{vdw}) had the largest contribution. On an average, contribution of van der Waals interaction energy was largest with -37.649Kcal/mol while coulomb energy (E_{coul}) also contributed a considerable value of -29.537Kcal/mol. The contributions of the other terms, lipophilic interaction (Lipo = -1.988), hydrogen bonding (hbond = -0.475), penalty for freezing rotatable bonds (E_{rotb} = 0.519) and term for polar interaction at active site (E_{site} = -0.148) were negligible. For, mutant complex the values were, -35.23Kcal/mol for van der Waals interaction energy, while coulomb energy (E_{coul}) also contributed a considerable value of -22.681Kcal/mol. The contributions of the other terms, lipophilic interaction (Lipo = -1.74), hydrogen bonding (hbond = -0.513), penalty for freezing rotatable bonds (E_{rotb} = 0.601) and term for polar interaction at active site (E_{site} = -0.108) .The division of the Glide score into various energy terms for both compounds is given in table 6.

In first complex, the oxygen of PPC was found to be making two hydrogen bonds with nitrogen of 134 Ala of PncA and the distance was 4.45Å and another with Asp8 and the distance was 4.53 Å. The ligand also made a significant number of hydrophobic bonds with Phe 13, leu 19, Val 21, Ile 133, His 137, Cys 138 and Val 163 of PncA (Figure 21). On, the other hand the mutant protein was found to be making three hydrogen bonds. The oxygen of the ligand was making hydrogen bonds with nitrogen of Ala 134 and Cys 138 and Asp8 and bond lengths were 2.55, 3.81and 2.68 Å rspectively with PPC. However in case of mutant protein there was less hydrophobic interaction than the native protein. The residues involved in hydrophobic interactions were Gln10, Phe13, Ile133, Ala134, Thr135, His 137 (Figure 22).

Complex	Glide Score		Glide Emodel	Potential Energy	Glide Eenergy
	HTVS	XP			
PPC-Wild	-5.935	-7.681	-105.435	128.341	-69.283
PPC-Mutant	-5.277	-8.183	-100.76	185.774	-65.091

Table 5: Binding affinity scores and energies of PPC in complex with native and mutant PncA

Complex	Lipo	hbond	E_{vdw}	E_{coul}	E_{rotb}	E_{site}
PPC-Wild	-1.988	-0.513	-37.649	-29.537	0.519	-0.148
PPC-Mutant	-1.74	-0.475	-35.23	-22.68	0.601	-0.108

Table 6: Division of Glide scores into its various components

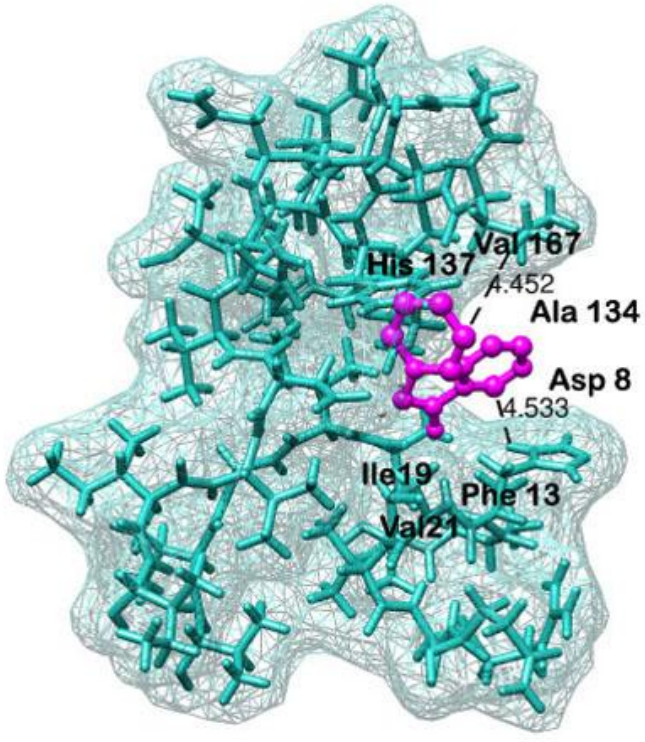

Figure 21: Interactions of native PncA with PPC

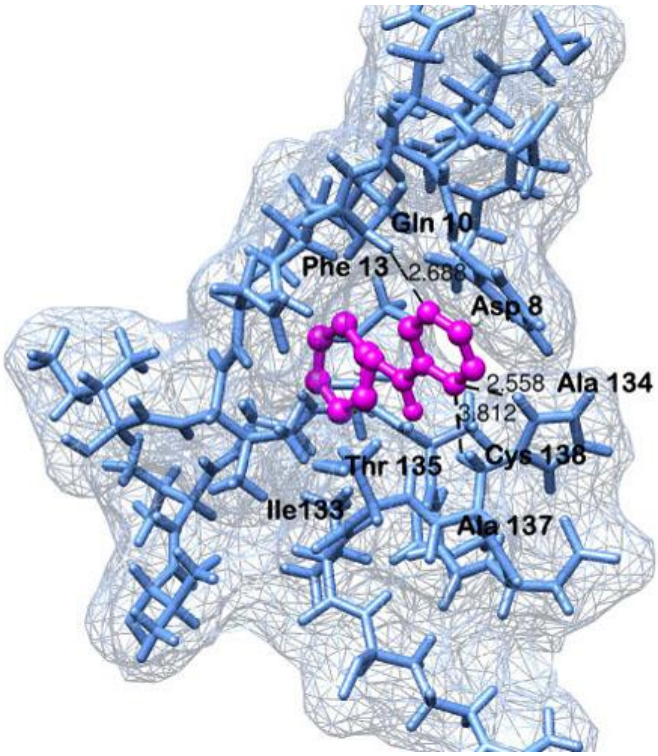

Figure 22: Interactions of mutant PncA with PPC

DISCUSSION

MDR TB or multi drug resistant tuberculosis is caused when resistance is developed for two or more 1st line drugs. Treatment of drug-resistant tuberculosis is hampered by poor efficacy and high toxicity of second-line drugs (Dooley et al., 2012).However, PZA is a pro-drug and acts only when metabolized by pyrazonic acid (POA). The enzyme pyrazonic acid is further derived from enzyme pyrazinamidase, encoded by *pncA* gene. Mycobacterial pyrazinamidase (MtPncA) is expressed in the cytoplasm and plays a pivotal role in the activation of pyrazinamide. This enzyme is expressed constitutively in the cytoplasm of M. Tuberculosis (Chang et al., 2011). Only after conversion of PZA into pyrazinoic acid by this enzyme the drug becomes potent. Destabilization of membrane potential and changes in the transport function are the underlying reasons for its bactericidal effect (Konno et al., 1967; Yeager et al., 1952; Zhang et al., 2008).

The PncA 3D-structure was available in PDB (3PLI). The structure has been determined to 2.2Å resolution using PhPncA by molecular replacement (Petrella et al., 2011). The structure consists of 185 residues as revealed by the X- ray crystallography. The six- stranded parallel beta sheets and two alpha helices are packed together and forms alpha/beta domain. The active site residue Cys138 is present in alpha- 3 helix which lies in the N-terminal region (Petrella et al., 2011). Site directed mutagenesis based experiments revealed Asp8, Lys96 and Cys138 to be the pivotal residues involved in catalysis and Asp49, His57 and His71 are metal ion binding residues. Mutations at these residues greatly affect the function of PncA enzyme (Du et al., 2001; Lemaitre et al., 1999; Petrella et al., 2011; Sheen et al., 2012).

One of the most prominent characteristics of the mutations identified from the data obtained from clinical isolates is their diversity. The mutations range from missense mutations to insertions and deletions and are spread throughout the *pncA* gene (Lemaitre et al., 2001; Ramaswamy and Musser, 1998; Scorpio et al., 1997). Since the drug is metabolized in acidic conditions, it becomes cumbersome to obtain reliable interpretation of data on resistance of M. Tuberculosis to the drug. Therefore, PCR amplification and DNA sequencing of *pncA* is an approach of interest as it allows rapid identification of the PncA mutations that may be involved in PZA resistance. This information can be used to study the correlation between structure and function i.e. to study the effects of mutation on the function of the enzyme. Mutation analysis could, thus be used to assess PZA susceptibility. Petrella et al and Sivashanmugam et al performed similar studies in PncA to identify the mechanism of resistance. They used docking studies coupled with molecular dynamics to establish their work. Several important inferences were made in the work. Petrella showed that it was hardening of the cavity which resulted in the loss of PZA activity. On the other hand, Sivashanmugam showed that no significant impact was made on the structure, however interaction pattern in wild and mutant varied significantly.

Purohit et al in 2013 performed a similar study targeting S315T in *Mycobacterium tuberculosis* catalase-peroxidase enzyme. Docking studies revealed that mutant (S315T) showed high docking score and INH binding affinity as compared to wild enzyme. However, in molecular dynamics simulation, mutant enzyme exhibited less structure fluctuation at INH

binding residues and more degree of fluctuation at C-terminal domain compared to wild enzyme. These computational studies and data endorse that MtBKatG mutation (S315T) decrease the flexibility of binding residues and made them rigid by altering the conformational changes, in turn it hampers the INH activity (Purohit et al., 2011).

Using the above studies as reference, in this study mutation a novel mutation Lys-96-Arg (K96R) is considered. This mutation has been revealed by deep sequencing via NGS (Next Generation sequencing) in the PncA gene of 26 random Multi Drug Resistant Tuberculosis patients of West African origin residing in USA. 9 out of 26 isolates were carrying this novel mutation making them resistant to pyrazinamide and in one case to all 1^{st} and 2^{nd} line drugs. The position spans the active centre of the protein and thereby is of utmost importance. Few mutations at Lys 96 have been previously studied making it a sought after topic of research round the world. Considering the ratio 9/26, the mutation seems to be quite prevalent. Since, tuberculosis is one of the most widespread disease, counteracting the causes of drug resistance via computational studies seems a good choice (Daum et al., 2014).

Here, we have tried to discover the answers targeting the questions raised by some recent researches. First, what are the structural changes produced by this mutation? Second, what is the mechanism of resistance of the drug due to this mutation? Therefore, in this study we have tried to identify how several properties are being affected by studying the physic-chemical characteristics. In the present work, we studied the relationship between structural and physico-chemical characteristics of PncA with mutation in the active site K96R and the enzymatic function and PZA resistance level of M. tuberculosis. Critical understanding of these mechanisms allows the development of robust and efficient molecular diagnostic tests and provides a platform for the development of new drugs. Further, knowledge of these mechanisms can help in developing precautionary measures to curb the development of resistance.

CONCLUSION AND FUTURE PERSPECTIVE

This study is intended to present a comprehensive analysis of the drug resistance mechanism by K96R mutation in the PncA enzyme of *M.tuberculosis*. In our research we have performed binding pocket analysis, molecular docking studies and 15ns molecular dynamics studies. The binding cavity results showed that the native PncA had a cavity volume of 551.9 $Å^3$ and mutant PncA had 1314.2 $Å^{3.}$ A very significant increase in the volume of the cavity makes the binding pocket extremely large thereby affecting the fitting of the lignad and its interactions with the protein considerably. From docking scores it was inferred that the native protein has significant complimentarity and interactions with the protein while in mutant the scores were less, indicating the low level of complimentarity. MD simulation of native and mutant gave the dynamic behaviour of the protein and mechanism of resistance after mutation. The altered behaviour of the protein was given by hydrogen bond interactions, RMSD, RMSF and radius of gyration. Hydrogen bonds of the ligand with the protein were reduced in mutant structure, suggesting less binding affinity compared to native. The RMSD for both native and mutant proteins were stable. RMSF and Radius of gyration plots were of great advantage in understanding the fluctuations. The plots confirmed that mutation caused the binding cavity to become enlarged. This resulted in a loosely bound ligand with fewer interactions with the protein and hindered the activation of PZA. We may conclude from our findings that K96R is a potential drug resistance causing mutation and should be considered while developing novel inhibitors targeting mutations in PncA. So, based on the findings a combinatorial library of pyrazinamide derivatives with 0.2 million compounds was created to identify potential leads. PPC was found to be an ideal candidate and good results were obtained with both wild and mutant PncA complexes.

For future studies, wet lab validation can be done for PPC as a potent drug candidate. The IC_{50} values can be calculated for PPC and compared to PZA. Further, modifications can be performed to make the drug even more potent. Apart from this, a series of PPC derivatives can be developed taking PPC as initial structure. Structure activity relationship can be performed. This study would be an important source of information for drug manufacturing companies. Computational QSAR can also be performed. These studies can identify what groups are significant. The development period can thus be considerably reduced by this. Effective drugs can thus be made available to general public at a competitive price. It has been widely established that TB is associated with poverty, overpopulation, and inadequate hygiene. With the current population trends (rapid growth in underdeveloped and aging in developed regions), the increased prevalence of poverty, the lack of access to clean water and sanitation, and the continued epidemic of AIDS, TB will continue to be one of the most important infectious agents in the near future. This approach would not only help to protect the efficacy of the current TB drugs but also boost the anti-TB activity of the existing TB- and non-TB drugs, ultimately broadening the therapeutic options for TB treatment.

REFERENCES

Andries, K., Verhasselt, P., Guillemont, J., Gohlmann, H.W., Neefs, J.M., Winkler, H., Van Gestel, J., Timmerman, P., Zhu, M., Lee, E.*, et al.* (2005). A diarylquinoline drug active on the ATP synthase of Mycobacterium tuberculosis. Science ***307***, 223-227.

Berman, H.M., Battistuz, T., Bhat, T.N., Bluhm, W.F., Bourne, P.E., Burkhardt, K., Feng, Z., Gilliland, G.L., Iype, L., Jain, S.*, et al.* (2002). The Protein Data Bank. Acta crystallographica. Section D, Biological crystallography ***58***, 899-907.

Buriankova, K., Doucet-Populaire, F., Dorson, O., Gondran, A., Ghnassia, J.C., Weiser, J., and Pernodet, J.L. (2004). Molecular basis of intrinsic macrolide resistance in the Mycobacterium tuberculosis complex. Antimicrobial agents and chemotherapy ***48***, 143-150.

Chang, K.C., Yew, W.W., and Zhang, Y. (2011). Pyrazinamide susceptibility testing in Mycobacterium tuberculosis: a systematic review with meta-analyses. Antimicrobial agents and chemotherapy ***55***, 4499-4505.

Dalton, T., Cegielski, P., Akksilp, S., Asencios, L., Campos Caoili, J., Cho, S.N., Erokhin, V.V., Ershova, J., Gler, M.T., Kazennyy, B.Y.*, et al.* (2012). Prevalence of and risk factors for resistance to second-line drugs in people with multidrug-resistant tuberculosis in eight countries: a prospective cohort study. Lancet ***380***, 1406-1417.

Daum, L.T., Fourie, P.B., Bhattacharyya, S., Ismail, N.A., Gradus, S., Maningi, N.E., Omar, S.V., and Fischer, G.W. (2014). Next-generation sequencing for identifying pyrazinamide resistance in Mycobacterium tuberculosis. Clinical infectious diseases : an official publication of the Infectious Diseases Society of America ***58***, 903-904.

Dietze, R., Hadad, D.J., McGee, B., Molino, L.P., Maciel, E.L., Peloquin, C.A., Johnson, D.F., Debanne, S.M., Eisenach, K., Boom, W.H.*, et al.* (2008). Early and extended early bactericidal activity of linezolid in pulmonary tuberculosis. American journal of respiratory and critical care medicine ***178***, 1180-1185.

Dooley, K.E., Mitnick, C.D., Ann DeGroote, M., Obuku, E., Belitsky, V., Hamilton, C.D., Makhene, M., Shah, S., Brust, J.C., Durakovic, N.*, et al.* (2012). Old drugs, new purpose: retooling existing drugs for optimized treatment of resistant tuberculosis. Clinical infectious diseases : an official publication of the Infectious Diseases Society of America ***55***, 572-581.

Dorman, S.E., and Chaisson, R.E. (2007). From magic bullets back to the magic mountain: the rise of extensively drug-resistant tuberculosis. Nature medicine ***13***, 295-298.

Du, X., Wang, W., Kim, R., Yakota, H., Nguyen, H., and Kim, S.H. (2001). Crystal structure and mechanism of catalysis of a pyrazinamidase from Pyrococcus horikoshii. Biochemistry ***40***, 14166-14172.

Dye, C. (2000). Tuberculosis 2000-2010: control, but not elimination. The international journal of tuberculosis and lung disease : the official journal of the International Union against Tuberculosis and Lung Disease ***4***, S146-152.

Ferrer, G., Acuna-Villaorduna, C., Escobedo, M., Vlasich, E., and Rivera, M. (2010). Outcomes of multidrug-resistant tuberculosis among binational cases in El Paso, Texas. The American journal of tropical medicine and hygiene ***83***, 1056-1058.

Friesner, R.A., Banks, J.L., Murphy, R.B., Halgren, T.A., Klicic, J.J., Mainz, D.T., Repasky, M.P., Knoll, E.H., Shelley, M., Perry, J.K*., et al.* (2004). Glide: a new approach for rapid, accurate docking and scoring. 1. Method and assessment of docking accuracy. J Med Chem ***47***, 1739-1749.

Golden, M.P., and Vikram, H.R. (2005). Extrapulmonary tuberculosis: an overview. American family physician ***72***, 1761-1768.

Heifets, L.B., and Cangelosi, G.A. (1999). Drug susceptibility testing of Mycobacterium tuberculosis: a neglected problem at the turn of the century State of the Art. The International Journal of Tuberculosis and Lung Disease ***3***, 564-581.

Hershkovitz, I., Donoghue, H.D., Minnikin, D.E., Besra, G.S., Lee, O.Y., Gernaey, A.M., Galili, E., Eshed, V., Greenblatt, C.L., Lemma, E*., et al.* (2008). Detection and molecular characterization of 9,000-year-old Mycobacterium tuberculosis from a Neolithic settlement in the Eastern Mediterranean. PloS one ***3***, 26-38.

Ito, K., Yamamoto, K., and Kawanishi, S. (1992). Manganese-mediated oxidative damage of cellular and isolated DNA by isoniazid and related hydrazines: non-Fenton-type hydroxyl radical formation. Biochemistry ***31***, 11606-11613.

Joe Dundas, Z.O., Jeffery Tseng, Andrew Binkowski, Yaron Turpaz, and Jie Liang . , (2006). CASTp: computed atlas of surface topography of proteins with structural and topographical mapping of functionally annotated resiudes. Nucleic Acid Research ***34***, W116-W118.

Jones, S., and Thornton, J.M. (1996). Principles of protein-protein interactions. Proceedings of the National Academy of Sciences of the United States of America ***93***, 13-20.

Jureen, P., Werngren, J., Toro, J.C., and Hoffner, S. (2008). Pyrazinamide resistance and pncA gene mutations in Mycobacterium tuberculosis. Antimicrobial agents and chemotherapy *52*, 1852-1854.
Konno, K., Feldmann, F.M., and McDermott, W. (1967). Pyrazinamide susceptibility and amidase activity of tubercle bacilli. The American review of respiratory disease ***95***, 461-469.

Koul, A., Vranckx, L., Dendouga, N., Balemans, W., Van den Wyngaert, I., Vergauwen, K., Gohlmann, H.W., Willebrords, R., Poncelet, A., Guillemont, J*., et al.* (2008). Diarylquinolines are bactericidal for dormant mycobacteria as a result of disturbed ATP homeostasis. The Journal of biological chemistry ***283***, 25273-25280.

Lemaitre, N., Callebaut, I., Frenois, F., Jarlier, V., and Sougakoff, W. (2001). Study of the structure-activity relationships for the pyrazinamidase (PncA) from Mycobacterium tuberculosis. The Biochemical journal ***353***, 453-458.

Lemaitre, N., Sougakoff, W., Truffot-Pernot, C., and Jarlier, V. (1999). Characterization of new mutations in pyrazinamide-resistant strains of Mycobacterium tuberculosis and identification of conserved regions important for the catalytic activity of the pyrazinamidase PncA. Antimicrobial agents and chemotherapy ***43***, 1761-1763.

Madhavi Sastry, G., Adzhigirey, M., Day, T., Annabhimoju, R., and Sherman, W. (2013). Protein and ligand preparation: parameters, protocols, and influence on virtual screening enrichments. J Comput Aided Mol Des ***27***, 221-234.

McQuade Billingsley, K., Smith, N., Shirley, R., Achieng, L., and Keiser, P. (2011). A quality assessment tool for tuberculosis control activities in resource limited settings. Tuberculosis ***91*** *Suppl 1*, S49-53.

Morlock, G.P., Crawford, J.T., Butler, W.R., Brim, S.E., Sikes, D., Mazurek, G.H., Woodley, C.L., and Cooksey, R.C. (2000). Phenotypic characterization of pncA mutants of Mycobacterium tuberculosis. Antimicrobial agents and chemotherapy ***44***, 2291-2295.

Pandey, S., Newton, S., Upton, A., Roberts, S., and Drinkovic, D. (2009). Characterisation of pncA mutations in clinical Mycobacterium tuberculosis isolates in New Zealand. Pathology ***41***, 582-584.
Petrella, S., Gelus-Ziental, N., Maudry, A., Laurans, C., Boudjelloul, R., and Sougakoff, W. (2011). Crystal structure of the pyrazinamidase of Mycobacterium tuberculosis: insights into natural and acquired resistance to pyrazinamide. PloS one ***6***, 157-175.

Purohit, R., Rajendran, V., and Sethumadhavan, R. (2011). Relationship between mutation of serine residue at 315th position in M. tuberculosis catalase-peroxidase enzyme and Isoniazid susceptibility: an in silico analysis. Journal of molecular modeling ***17***, 869-877.

Rajendran, V., and Sethumadhavan, R. (2014). Drug resistance mechanism of PncA in Mycobacterium tuberculosis. Journal of biomolecular structure & dynamics ***32***, 209-221.

Ramaswamy, S., and Musser, J.M. (1998). Molecular genetic basis of antimicrobial agent resistance in Mycobacterium tuberculosis: 1998 update. Tubercle and lung disease : the official journal of the International Union against Tuberculosis and Lung Disease ***79***, 3-29.

Rao, S.P., Alonso, S., Rand, L., Dick, T., and Pethe, K. (2008). The protonmotive force is required for maintaining ATP homeostasis and viability of hypoxic, nonreplicating Mycobacterium tuberculosis. Proceedings of the National Academy of Sciences of the United States of America ***105***, 11945-11950.

Rustomjee, R., Diacon, A.H., Allen, J., Venter, A., Reddy, C., Patientia, R.F., Mthiyane, T.C., De Marez, T., van Heeswijk, R., Kerstens, R.*, et al.* (2008). Early bactericidal activity and pharmacokinetics of the diarylquinoline TMC207 in treatment of pulmonary tuberculosis. Antimicrobial agents and chemotherapy ***52***, 2831-2835.

Schrödinger Release 2013-1: Desmond Molecular Dynamics System, v., D. E. Shaw Research, New York, NY, 2013. Maestro-Desmond Interoperability Tools, version 3.4, Schrödinger, New York, NY, 2013.

Schrödinger Release 2013-1: LigPrep, v., Schrödinger, LLC, New York, NY, 2013.

Schrödinger Release 2013-1: Schrödinger Suite 2013 Protein Preparation Wizard; Epik version 2.4, S., LLC, New York, NY, 2013; Impact version 5.9, Schrödinger, LLC, New York, NY, 2013; Prime version 3.2, Schrödinger, LLC, New York, NY, 2013.

Scorpio, A., Lindholm-Levy, P., Heifets, L., Gilman, R., Siddiqi, S., Cynamon, M., and Zhang, Y. (1997). Characterization of pncA mutations in pyrazinamide-resistant Mycobacterium tuberculosis. Antimicrobial agents and chemotherapy ***41***, 540-543.

Scorpio, A., and Zhang, Y. (1996). Mutations in pncA, a gene encoding pyrazinamidase/nicotinamidase, cause resistance to the antituberculous drug pyrazinamide in tubercle bacillus. Nature medicine ***2***, 662-667.

Sethumadhavan, V.R.R. (2014). Drug resistance mechanism of PncA in Mycobacterium tuberculosis. Journal of Biomolecular Structure and Dynamics ***32***, 209-221.

Shaw, K.J., and Barbachyn, M.R. (2011). The oxazolidinones: past, present, and future. Annals of the New York Academy of Sciences ***1241***, 48-70.

Sheen, P., Ferrer, P., Gilman, R.H., Christiansen, G., Moreno-Roman, P., Gutierrez, A.H., Sotelo, J., Evangelista, W., Fuentes, P., Rueda, D*., et al.* (2012). Role of metal ions on the activity of Mycobacterium tuberculosis pyrazinamidase. The American journal of tropical medicine and hygiene ***87***, 153-161.

Shi, W., Zhang, X., Jiang, X., Yuan, H., Lee, J.S., Barry, C.E., 3rd, Wang, H., Zhang, W., and Zhang, Y. (2011). Pyrazinamide inhibits trans-translation in Mycobacterium tuberculosis. Science ***333***, 1630-1632.

Shivakumar, D., Williams, J., Wu, Y., Damm, W., Shelley, J., and Sherman, W. (2010). Prediction of Absolute Solvation Free Energies using Molecular Dynamics Free Energy Perturbation and the OPLS Force Field. Journal of Chemical Theory and Computation ***6***, 1509-1519.

Sivashanmugam M, e.a., Lakshmipathy D, Ramasubban G, Therese L, Vetrivel U, Sivashanmugam M, et al. (2013). In silico Analysis of Novel Mutation ala102pro Targeting pncA Gene of M. Tuberculosis. J Comput Sci Syst Biol ***6***, 083-087.

Small-Molecule Drug Discovery Suite 2013-1: Glide, v., Schrödinger, LLC, New York, NY, 2013.

Smith, T., Wolff, K.A., and Nguyen, L. (2013). Molecular biology of drug resistance in Mycobacterium tuberculosis. Current topics in microbiology and immunology ***374***, 53-80.

Sreevatsan, S., Pan, X., Zhang, Y., Kreiswirth, B.N., and Musser, J.M. (1997). Mutations associated with pyrazinamide resistance in pncA of Mycobacterium tuberculosis complex organisms. Antimicrobial agents and chemotherapy ***41***, 636-640.

Vetting, M., Roderick, S.L., Hegde, S., Magnet, S., and Blanchard, J.S. (2003). What can structure tell us about in vivo function? The case of aminoglycoside-resistance genes. Biochemical Society transactions ***31***, 520-522.

Wang, J.Y., Burger, R.M., and Drlica, K. (1998). Role of superoxide in catalase-peroxidase-mediated isoniazid action against mycobacteria. Antimicrobial agents and chemotherapy ***42***, 709-711.

Wei, J., Dahl, J.L., Moulder, J.W., Roberts, E.A., O'Gaora, P., Young, D.B., and Friedman, R.L. (2000). Identification of a Mycobacterium tuberculosis gene that enhances mycobacterial survival in macrophages. Journal of bacteriology ***182***, 377-384.

Wishart, D.S., Knox, C., Guo, A.C., Cheng, D., Shrivastava, S., Tzur, D., Gautam, B., and Hassanali, M. (2008). DrugBank: a knowledgebase for drugs, drug actions and drug targets. Nucleic acids research ***36***, D901-906.

Wright, A., Zignol, M., Van Deun, A., Falzon, D., Gerdes, S.R., Feldman, K., Hoffner, S., Drobniewski, F., Barrera, L., van Soolingen, D*., et al.* (2009). Epidemiology of antituberculosis drug resistance 2002-07: an updated analysis of the Global Project on Anti-Tuberculosis Drug Resistance Surveillance. Lancet ***373***, 1861-1873.

Yeager, R.L., Munroe, W.G., and Dessau, F.I. (1952). Pyrazinamide (aldinamide) in the treatment of pulmonary tuberculosis. American review of tuberculosis ***65***, 523-546.

Zhang, H., Deng, J.Y., Bi, L.J., Zhou, Y.F., Zhang, Z.P., Zhang, C.G., Zhang, Y., and Zhang, X.E. (2008). Characterization of Mycobacterium tuberculosis nicotinamidase/pyrazinamidase. The FEBS journal ***275***, 753-762.

Zhang, Y., and Yew, W.W. (2009). Mechanisms of drug resistance in Mycobacterium tuberculosis. The international journal of tuberculosis and lung disease : the official journal of the International Union against Tuberculosis and Lung Disease ***13***, 1320-1330.

APPENDIX

RMSD Table

Time (ps)	RMSD_Mutant Unbound	RMSD_Mutant Bound	RMSD_Native Bound
0	5.38E-15	9.49E-15	7.58E-15
680.136	1.4425	2.068312	1.100872
1320.264	1.04854	2.554447	1.069622
1960.392	1.80055	2.637594	1.281534
2600.52	1.530564	3.120883	1.292226
3240.648	1.650965	2.815565	1.548191
3880.776	2.021387	2.895543	1.433529
4520.904	1.929925	3.123574	1.447105
5161.032	2.180469	4.109868	1.524744
5801.16	2.758902	3.809318	1.330258
6441.288	3.073921	3.84318	1.283444
7081.416	2.263475	3.479007	1.530044
7721.544	3.033556	3.956662	1.438913
8361.672	3.653187	3.690938	1.508206
9001.8	3.044333	3.714272	1.721721
9641.928	3.486808	4.110677	1.613177
10282.06	2.917448	3.609153	1.43471
10922.18	3.905681	4.174358	1.467049
11562.31	3.410691	4.169012	1.438436
12202.44	3.125598	3.144637	1.41108
12842.57	3.029493	3.800587	1.368278
13482.7	2.976035	3.40838	1.473585
14122.82	3.32085	4.333809	1.407524
14762.95	3.337148	4.910861	1.730523
15000	2.8092004	5.137051	1.55

RMSF Table

Residue Number	RMSF_Native Bound	RMSF_Mutant Unbound	RMSF_Mutant Bound
1	1.165174	1.084888	3.110904
2	0.601622	0.791778	1.377921
3	0.487678	0.582971	0.656973
4	0.412933	0.445078	0.486475
5	0.389604	0.467526	0.435555
6	0.482677	0.515752	0.436566
7	0.491471	0.635811	0.510352
8	0.635117	0.795579	0.640646
9	0.562294	0.796608	0.890527
10	0.544172	1.07091	1.114127
11	0.464324	1.24373	1.48289
12	0.517457	1.213755	1.912549
13	0.572594	0.948946	2.254232
14	0.704673	1.104201	1.71058
15	0.941369	1.317562	1.521266
16	1.101465	1.620704	1.644613
17	0.849067	1.454655	2.264007
18	1.026527	1.716063	2.417749
19	0.819958	1.403191	3.226318
20	0.737193	1.2654	2.821722
21	0.651043	1.274207	2.375324
22	0.993383	2.096357	1.989849
23	0.992907	2.615907	2.231889
24	0.738645	2.393464	2.059542
25	0.734978	1.791576	1.829424
26	0.756232	1.742985	1.622219
27	0.652182	1.516064	1.808253
28	0.67661	1.653752	1.777635
29	0.710323	1.779501	1.93792
30	0.615307	2.049669	2.07103

31	0.718121	1.935393	2.43719
32	0.910046	1.696488	2.185344
33	0.88543	1.767139	1.671384
34	0.711667	1.247559	1.804253
35	1.039663	1.135652	1.382601
36	1.521696	1.626574	1.365968
37	2.104659	1.585523	1.812512
38	2.271396	1.178012	1.880808
39	1.777294	1.017061	1.523896
40	1.326546	0.969486	1.448675
41	0.703348	0.759183	1.222663
42	0.586591	0.745317	0.77073
43	0.649866	0.625839	0.723707
44	0.53752	0.512103	0.642643
45	0.431666	0.504125	0.529637
46	0.484843	0.616343	0.494515
47	0.524491	0.695155	0.553416
48	0.559996	0.87602	0.604043
49	0.597354	1.155584	0.669237
50	0.667384	1.202669	0.711293
51	0.523629	1.251361	0.750848
52	0.646268	1.554156	0.785902
53	0.655046	1.965284	1.143862
54	0.685529	2.810438	1.307439
55	0.803369	2.988842	1.284697
56	0.871068	3.193562	1.665683
57	0.716646	3.527403	1.913811
58	0.692454	2.895956	1.672305
59	0.881965	2.910707	1.785551
60	1.229574	3.393751	2.508599
61	1.221234	4.62573	3.352674
62	1.141506	5.195828	3.568167
63	1.278959	5.971602	3.43328
64	1.303678	5.224419	3.793418

65	1.389572	5.961722	3.610196
66	1.149715	5.701545	3.60743
67	0.929273	4.671693	2.966625
68	0.804714	3.37918	2.678003
69	0.824387	2.496487	2.369722
70	0.73001	1.757189	2.322944
71	0.54458	1.24394	1.929022
72	0.468409	1.457895	1.592999
73	0.603169	1.35029	1.277824
74	0.874534	1.785583	1.232365
75	1.345825	2.481293	1.564967
76	0.898734	1.92917	2.24351
77	0.735721	1.733761	1.874496
78	0.634253	1.507888	2.051273
79	0.589702	1.339245	1.799956
80	0.588689	1.173579	1.383588
81	0.604626	0.909023	1.409174
82	0.565319	0.885289	1.324647
83	0.793085	1.557965	1.314344
84	0.982021	2.199178	1.538453
85	1.090363	1.74763	1.779534
86	1.592518	1.951583	1.686886
87	1.59728	1.546048	1.950814
88	1.442577	1.336864	1.633312
89	1.180493	0.998104	1.501618
90	0.704914	0.67856	1.112249
91	0.624949	0.644639	0.755368
92	0.567491	0.655079	0.716045
93	0.607524	0.759188	0.71073
94	0.614142	0.773026	0.770196
95	0.527579	0.928283	0.659274
96	0.546868	1.066629	0.689637
97	0.587151	1.307017	0.780201
98	0.613132	1.686704	0.83283

99	0.690273	2.352897	0.905918
100	0.711719	2.099796	1.301039
101	0.757925	1.913807	1.176241
102	0.787574	1.906041	1.299097
103	0.71128	2.351023	1.313038
104	0.633238	1.644976	1.183553
105	0.632979	1.398652	0.883079
106	0.684674	1.124302	0.786189
107	0.667541	1.207049	0.800573
108	0.676443	1.068891	0.895792
109	0.521466	0.952378	0.824209
110	0.611737	0.903338	0.688871
111	0.832112	1.024255	0.783046
112	0.908597	1.105718	0.962568
113	0.776451	1.142521	1.038042
114	0.668113	1.065926	0.943942
115	0.56628	1.020952	0.825545
116	0.542575	0.910197	0.746313
117	0.565104	1.027105	0.673036
118	0.559974	1.097222	0.761105
119	0.479439	0.968537	0.800465
120	0.477974	0.915265	0.69548
121	0.612717	1.096754	0.652801
122	0.718235	1.14951	0.835183
123	0.741006	1.108621	0.942083
124	0.757317	1.177312	0.835561
125	0.612662	0.962948	0.87534
126	0.633613	0.909991	0.689393
127	0.499117	0.771826	0.671732
128	0.437959	0.603885	0.535785
129	0.411996	0.469425	0.46709
130	0.467838	0.516814	0.403438
131	0.445298	0.533514	0.505036
132	0.482573	0.693215	0.553081

133	0.496256	0.858351	0.734122
134	0.5135	0.99094	0.84011
135	0.544632	1.013365	0.91584
136	0.67511	1.285929	0.914196
137	0.511374	1.285049	1.082021
138	0.476051	0.988013	0.947223
139	0.446139	0.802452	0.731542
140	0.487802	0.931305	0.644681
141	0.565698	1.045592	0.722602
142	0.494585	0.856206	0.79554
143	0.518836	0.838467	0.669161
144	0.623638	1.04215	0.646069
145	0.587943	1.056947	0.777971
146	0.549297	0.903101	0.818055
147	0.719218	0.956133	0.661238
148	0.803199	1.137101	0.781693
149	0.772274	1.152692	0.975249
150	0.817632	1.116582	0.954092
151	0.592316	0.906971	0.946159
152	0.541464	0.795165	0.687957
153	0.48512	0.699176	0.601554
154	0.447256	0.58178	0.539934
155	0.415937	0.584061	0.491154
156	0.440935	0.576201	0.529708
157	0.598672	0.742521	0.58074
158	0.650545	0.787351	0.78545
159	0.585299	0.68486	0.887016
160	0.595879	0.766114	0.985517
161	0.858454	0.941725	0.879482
162	0.93395	1.163166	0.967943
163	0.768371	1.357101	1.135907
164	0.958852	1.438602	1.473671
165	1.27366	1.561038	1.530625
166	1.469845	1.579929	1.661406

167	1.235346	1.423046	1.669212
168	0.936799	1.291711	1.472796
169	0.965171	1.391842	1.294029
170	0.939986	1.471036	1.364217
171	0.729523	1.222658	1.3026
172	0.689158	1.028105	1.003558
173	0.790975	1.093829	0.947743
174	0.784729	1.140864	1.097775
175	0.611654	0.952134	1.060873
176	0.698549	0.934866	0.836076
177	0.834175	1.079208	0.952187
178	0.736402	1.068805	1.164214
179	0.653158	0.950598	1.074479
180	0.530675	0.789311	0.93536
181	0.515762	0.706123	0.72203
182	0.595481	0.768622	0.663354
183	0.604122	0.796769	0.769475
184	0.755721	1.061922	0.750785
185	0.919451	1.464219	0.929753

Radius of Gyration Data

Time(ps)	Rg_Native Bound	Rg_Mutant Bound
0	15.36316	15.86572
640.128	15.41075	16.1172
1280.256	15.43839	16.00847
1920.384	15.54645	16.2486
2560.512	15.43726	16.16699
3200.64	15.47265	16.29492
3840.768	15.40231	16.10731
4480.896	15.49079	16.26758
5121.024	15.44701	16.23167
5761.152	15.46517	16.50512
6401.28	15.46082	16.90991
7041.408	15.57381	16.66998
7681.536	15.44749	16.49041
8321.664	15.48787	16.48132
8961.792	15.37386	16.55745
9601.92	15.50826	16.26114
10242.05	15.44394	16.25848
10882.18	15.51671	15.82392
11522.3	15.52966	16.25285
12162.43	15.52814	16.0446
12802.56	15.58611	16.27486
13442.69	15.47956	16.18597
14082.82	15.5224	16.44954
14722.94	15.54459	16.56436
15000	15.45811	16.60369

HTVS Data for wild PncA

Title	Docking Score	Glide Evdw	Glide Ecoul	Glide Emodel	Glide Energy
TEMP00078025	-8.93576	-37.649766	-29.537654	-105.43596	-69.283437
TEMP00753783	-8.375469	-34.990006	-15.969659	-89.608838	-50.959664
TEMP32123916	-8.350259	-39.042722	-8.668116	-71.342838	-47.710837
TEMP13485957	-8.319413	-13.478953	-12.802529	-40.085129	-26.281482
TEMP14610071	-8.304906	-30.471122	-12.506413	-63.27382	-42.977534
TEMP14811023	-8.298324	-35.008665	-11.577007	-62.400938	-46.585672
TEMP01147568	-8.221512	-45.334257	-5.605367	-75.159529	-50.939624
TEMP13517187	-7.183744	-33.493675	-8.404621	-60.374985	-41.898296
TEMP05158373	-7.281754	-29.058864	-3.182855	-41.782785	-32.24172
TEMP05158373	-7.281754	-29.058864	-3.182855	-41.782785	-32.24172
TEMP68604214	-7.281569	-18.990282	-12.834154	-40.204981	-31.824437
TEMP02385218	-7.281544	-27.21536	-10.825198	-50.267473	-38.040558
TEMP15959517	-7.281494	-34.662884	-0.483873	-45.530371	-35.146756
TEMP01531503	-7.281462	-25.29574	-0.224345	-33.313927	-25.520086
TEMP68572994	-7.281439	-19.604959	-0.909645	-25.671146	-20.514604
TEMP19701932	-7.281386	-28.951703	-2.704991	-41.72218	-31.656694
TEMP67911817	-7.281379	-29.864433	-18.025375	-58.902286	-47.889808
TEMP13731490	-7.281339	-28.455533	-0.837396	-40.778988	-29.292929
TEMP70454675	-5.281194	-29.627443	-4.4166	-42.462882	-34.044044
TEMP19323209	-5.281045	-11.219063	-25.257348	-41.529468	-36.476411
TEMP04267417	-5.280901	-17.564538	-2.008938	-25.72021	-19.573476
TEMP04291979	-5.280897	-31.341105	-1.258093	-43.320391	-32.599197
TEMP14610071	-5.280897	-31.341105	-1.258093	-43.320391	-32.599197
TEMP03852160	-5.280874	-28.916206	-4.8843	-43.768728	-33.800506
TEMP11866342	-5.280832	-28.333962	-9.801055	-47.891012	-38.135017
TEMP00488896	-5.280808	-21.609566	-1.610006	-31.19337	-23.219572
TEMP59587150	-5.280773	-24.917774	-4.841588	-41.120253	-29.759362
TEMP03153945	-5.280656	-25.755831	-7.67302	-45.365144	-33.428851

HTVS Data for mutant PncA

Title	Docking Score	Glide Evdw	Glide Ecoul	Glide Emodel	Glide Energy
TEMP00078025	-8.277543	-35.238600	-22.686892	-100.7621	-65.0918
TEMP32123916	-8.375469	-34.990006	-15.969659	-89.6088	-50.9597
TEMP00753784	-8.350259	-39.042722	-8.668116	-71.3428	-47.7108
TEMP13485957	-8.319413	-13.478953	-12.802529	-40.0851	-26.2815
TEMP14610071	-8.304906	-30.471122	-12.506413	-63.2738	-42.9775
TEMP14811023	-8.298324	-35.008665	-11.577007	-62.4009	-46.5857
TEMP01147568	-8.221512	-45.334257	-5.605367	-75.1595	-50.9396
TEMP03066341	-8.183744	-33.493675	-8.404621	-60.375	-41.8983
TEMP01149997	-8.181719	-41.901379	-6.691125	-73.3983	-48.5925
TEMP68582612	-8.153378	-32.530361	-7.34754	-56.7526	-39.8779
TEMP03844868	-8.149798	-38.2046	-8.258777	-69.8186	-46.4634
TEMP01295738	-8.103758	-42.896983	-3.45112	-65.4835	-46.3481
TEMP03869607	-8.043957	-27.732891	-14.707493	-63.5406	-42.4404
TEMP00303502	-8.035032	-33.395277	-4.243574	-53.7122	-37.6389
TEMP00088576	-8.03415	-27.397455	-4.714377	-47.8822	-32.1118
TEMP01114961	-8.016459	-29.797466	-4.803605	-52.5567	-34.6011
TEMP04024310	-8.008715	-28.866356	-6.73307	-44.6388	-35.5994
TEMP13322012	-7.988322	-41.623437	-8.062585	-70.9012	-49.686
TEMP00803236	-7.974016	-40.94557	-6.468982	-73.1013	-47.4146
TEMP35455039	-7.949333	-21.26805	-24.264869	-64.353	-45.5329
TEMP35455039	-7.949333	-21.26805	-24.264869	-64.353	-45.5329
TEMP00129954	-7.940722	-31.83122	-10.409254	-62.9567	-42.2405
TEMP13121745	-7.931469	-40.215306	-3.856813	-63.1895	-44.0721
TEMP08254174	-7.892621	-32.533049	-4.711894	-54.1405	-37.2449
TEMP40309647	-7.830812	-40.489017	-11.096663	-75.8515	-51.5857
TEMP02038927	-7.820249	-36.304012	-17.558382	-88.1542	-53.8624
TEMP12636976	-7.819499	-27.622916	-10.01987	-51.7999	-37.6428
TEMP02133968	-7.800787	-27.153165	-6.285074	-47.5867	-33.4382